Mitochondrial respiratory states and rates:
Building blocks of mitochondrial physiology Part 1

Corresponding author: Gnaiger E
Co-authors:
Aasander Frostner E, Abumrad NA, Acuna-Castroviejo D, Ahn B, Ali SS, Alves MG, Amati F, Aral C, Arandarčikaitė O, Bailey DM, Bajpeyi S, Bakker BM, Bastos Sant'Anna Silva AC, Battino M, Bazil J, Beard DA, Bednarczyk P, Ben-Shachar D, Bergdahl A, Bernardi P, Bishop D, Blier PU, Boetker HE, Boros M, Borsheim E, Borutaitė V, Bouillaud F, Bouitbir J, Breton S, Brown DA, Brown GC, Brown RA, Brozinick JT, Buettner GR, Burtscher J, Calabria E, Calbet JA, Calzia E, Cannon DT, Canto AC, Cardoso LHD, Carvalho E, Casado Pinna M, Cassina AM, Castro L, Cavalcanti-de-Albuquerque JP, Cervinkova Z, Chaurasia B, Chen Q, Chicco AJ, Chinopoulos C, Chowdhury SK, Clementi E, Coen PM, Coker RH, Collin A, Crisóstomo L, Darveau CA, Das AM, Dash RK, Davis MS, De Palma C, Dembinska-Kiec A, Dias TR, Distefano G, Doerrier C, Drahota Z, Dubouchaud H, Duchen MR, Dumas JF, Durham WJ, Dymkowska D, Dyrstad SE, Dzialowski EM, Ehinger J, Elmer E, Endlicher R, Engin AB, Fell DA, Ferko M, Ferreira JCB, Ferreira R, Fessel JP, Filipovska A, Fisar Z, Fischer M, Fisher G, Fisher JJ, Fornaro M, Galkin A, Gan Z, Garcia-Roves PM, Garcia-Souza LF, Garlid KD, Garrabou G, Garten A, Gastaldelli A, Genova ML, Giovarelli M, Gonzalez-Armenta JL, Gonzalo H, Goodpaster BH, Gorr TA, Gourlay CW, Granata C, Grefte S, Gueguen N, Haas CB, Haavik J, Haendeler J, Hamann A, Han J, Hancock CR, Hand SC, Hargreaves IP, Harrison DK, Heales SJR, Hellgren KT, Hepple RT, Hernansanz-Agustin P, Hickey AJ, Hoel F, Holland OJ, Holloway GP, Hoppel CL, Houstek J, Hunger M, Iglesias-Gonzalez J, Irving BA, Iyer S, Jackson CB, Jadiya P, Jang DH, Jang YC, Jansen-Dürr P, Jespersen NR, Jha RK, Jurk D, Kaambre T, Kaczor JJ, Kainulainen H, Kandel SM, Kane DA, Kappler L, Karabatsiakis A, Karkucinska-Wieckowska A, Keijer J, Keppner G, Khamoui AV, Klingenspor M, Komlodi T, Koopman WJH, Kopitar-Jerala N, Kowaltowski AJ, Krajcova A, Krako Jakovljevic N, Kristal BS, Kuang J, Kucera O, Kwak HB, Kwast K, Labieniec-Watala M, Lai N, Land JM, Lane N, Laner V, Lanza IR, Larsen TS, Lavery GG, Lee HK, Leeuwenburgh C, Lemieux H, Lerfall J, Li PA, Liu J, Lucchinetti E, Macedo MP, MacMillan-Crow LA, Makrecka-Kuka M, Malik A, Markova M, Martin DS, Mazat JP, McKenna HT, Menze MA, Meszaros AT, Methner A, Michalak S, Moellering DR, Moisoi N, Molina AJA, Montaigne D, Moore AL, Moreau K, Moreno-Sánchez R, Moreira BP, Mracek T, Muntane J, Muntean DM, Murray AJ, Nair KS, Nemec M, Neufer PD, Neuzil J, Newsom S, Nozickova K, O'Gorman D, Oliveira MF, Oliveira MT, Oliveira PF, Oliveira PJ, Orynbayeva Z, Osiewacz HD, Pak YK, Pallotta ML, Palmeira CM, Parajuli N, Passos JF, Patel HH, Pecina P, Pelnena D, Pereira da Silva Grilo da Silva F, Pesta D, Petit PX, Pettersen IKN, Pichaud N, Piel S, Pietka TA, Pino MF, Pirkmajer S, Porter C, Porter RK, Pranger F, Prochownik EV, Pulinilkunnil T, Puskarich MA, Puurand M, Quijano C, Radenkovic F, Radi R, Ramzan R, Rattan S, Reboredo P, Renner-Sattler K, Robinson MM, Roden M, Rodríguez-Enriquez S, Rohlena J, Rolo AP, Ropelle ER, Røsland GV, Rossiter HB, Rybacka-Mossakowska J, Saada A, Safaei Z, Salin K, Salvadego D, Sandi C, Sanz A, Sazanov LA, Scatena R, Schartner M, Scheibye-Knudsen M, Schilling JM, Schlattner U, Schönfeld P, Schwarzer C, Scott GR, Shabalina IG, Sharma P, Sharma V, Shevchuk I, Siewiera K, Silber AM, Silva AM, Sims CA, Singer D, Skolik R, Smenes BT, Smith J, Soares FAA, Sobotka O, Sokolova I, Sonkar VK, Sparagna GC, Sparks LM, Spinazzi M, Stankova P, Stary C, Stiban J, Stier A, Stocker R, Sumbalova Z, Suravajhala P, Swerdlow RH, Swiniuch D, Szabo I, Szewczyk A, Tanaka M, Tandler B, Tarnopolsky MA, Tavernarakis N, Tepp K, Thyfault JP, Tomar D, Towheed A, Tretter L, Trifunovic A, Trivigno C, Tronstad KJ, Trougakos IP, Tyrrell DJ, Urban T, Valentine JM, Velika B, Vendelin M, Vercesi AE, Victor VM, Vieyra A

52   Villena JA, Vitorino RMP, Vogt S, Volani C, Votion DM, Vujacic-Mirski K, Wagner BA,
53   Ward ML, Warnsmann V, Wasserman DH, Watala C, Wei YH, Wieckowski MR, Williams
54   C, Wohlgemuth SE, Wohlwend M, Wolff J, Wüst RCI, Yokota T, Zablocki K, Zaugg K,
55   Zaugg M, Zhang Y, Zhang YZ, Zischka H, Zorzano A

56

64

103

Abstract As the knowledge base and importance of mitochondrial physiology to human health expands, the necessity for harmonizing the terminology concerning mitochondrial respiratory states and rates has become increasingly apparent. The chemiosmotic theory establishes the mechanism of energy transformation and coupling in oxidative phosphorylation. The unifying concept of the protonmotive force provides the framework for developing a consistent theoretical foundation of mitochondrial physiology and bioenergetics. We follow IUPAC guidelines on terminology in physical chemistry, extended by considerations on open systems and irreversible thermodynamics. The concept-driven constructive terminology incorporates the meaning of each quantity and aligns concepts and symbols to the nomenclature of classical bioenergetics. In the frame of COST Action MitoEAGLE open to global bottom-up input, we endeavour to provide a balanced view on mitochondrial respiratory control and a critical discussion on reporting data of mitochondrial respiration in terms of metabolic flows and fluxes. Uniform standards for evaluation of respiratory states and rates will ultimately support the development of databases of mitochondrial respiratory function in species, tissues, and cells. Clarity of concept and consistency of nomenclature facilitate effective transdisciplinary communication, education, and ultimately further discovery.

Executive summary

1. In view of the broad implications for health care, mitochondrial researchers face an increasing responsibility to disseminate their fundamental knowledge and novel discoveries to a wide range of stakeholders and scientists beyond the group of specialists. This requires implementation of a commonly accepted terminology within the discipline and standardization in the translational context. Authors, reviewers, journal editors, and lecturers are challenged to collaborate with the aim to harmonize the nomenclature in the growing field of mitochondrial physiology and bioenergetics, from evolutionary biology and comparative physiology to mitochondrial medicine.

2. Aerobic respiration depends on the coupling of phosphorylation (ADP $\rightarrow$ ATP) to O_2 flux in catabolic reactions. Coupling in oxidative phosphorylation is mediated by translocation of protons across the inner mitochondrial membrane through proton pumps generating or utilizing the protonmotive force, that is measured between the mitochondrial matrix and intermembrane compartment or outer mitochondrial space. Compartmental coupling distinguishes vectorial oxidative phosphorylation from glycolytic fermentation as the counterpart of cellular core energy metabolism (**Figure 1**).

3. To exclude fermentation and other cytosolic interactions from exerting an effect on the analysis of mitochondrial metabolism, the barrier function of the plasma membrane must be disrupted. Selective removal or permeabilization of the plasma membrane yields mitochondrial preparations—including isolated mitochondria, tissue and cellular preparations—with structural and functional integrity. Then extra-mitochondrial concentrations of fuel substrates, ADP, ATP, inorganic phosphate, and cations including H^+ can be controlled to determine mitochondrial function under a set of conditions defined as coupling control states. A concept-driven terminology of bioenergetics explicitly incorporates in its terms and symbols information on the nature of respiratory states that makes the technical terms readily recognized and more easy to understand.

Figure 1. Mitochondrial respiration is the oxidation of fuel substrates (electron donors) and reduction of O_2 catalysed by the electron transfer system, ETS: (*a*) mitochondrial catabolic respiration; (*b*) mitochondrial and non-mitochondrial catabolic O_2 consumption; O_2 balance of (*c*) total cellular O_2 consumption and (*d*) external respiration


All chemical reactions, r, that consume O_2 in the cells of an organism, contribute to cell respiration, J_{rO_2}. ❶ Non-mitochondrial O_2 consumption by catabolic reactions, particularly peroxisomal oxidases and microsomal cytochrome P450 systems; ❷ mitochondrial residual oxygen consumption, *Rox*, after blocking the ETS; ❸ non-mitochondrial *Rox*; ❹ extracellular O_2 consumption; ❺ aerobic microbial respiration. Bars are not at a quantitative scale.

a **Mitochondrial catabolic respiration**, J_{kO_2}, is the O_2 consumption by the mitochondrial ETS maintaining the protonmotive force, Δp. J_{kO_2} excludes *Rox*.

b **Catabolic respiration** is the O_2 consumption associated with catabolic pathways in the cell, including peroxisomal and microsomal oxidation reactions (❶) in addition to mitochondrial catabolism (* The reactions k have to be defined specifically for *a* and *b*.)

c **Cell respiration**, J_{rO_2}, takes into account internal O_2-consuming reactions, r, including catabolic respiration and *Rox*. Internal respiration of an organism includes extracellular O_2 consumption (❹) and aerobic respiration by the microbiome (❺). Respiration is distinguished from fermentation by: (*1*) External electron acceptors for the maintenance of redox balance, whereas fermentation is characterized by an internal electron acceptor produced in intermediary metabolism. In aerobic cell respiration, redox balance is maintained by O_2 as the electron acceptor. (*2*) Compartmental coupling in vectorial oxidative phosphorylation, in contrast to exclusively scalar substrate-level phosphorylation in fermentation.

d **External respiration** balances internal respiration at steady-state. O_2 is transported from the environment across the respiratory cascade (circulation between tissues and diffusion across cell membranes) to the intracellular compartment, while bicarbonate and CO_2 are transported in reverse to the extracellular mileu and the organismic environment. Hemoglobin provides the molecular paradigm for the combination of O_2 and CO_2 exchange, as do lungs and gills on the morphological level. The respiratory quotient, *RQ*, is the molar CO_2/O_2 exchange ratio; when combined with the respiratory nitrogen quotient, N/O_2 (mol N given off per mol O_2 consumed), the *RQ* reflects the proportion of carbohydrate, lipd and protein utilized in cell respiration during aerobically balanced steady-states.
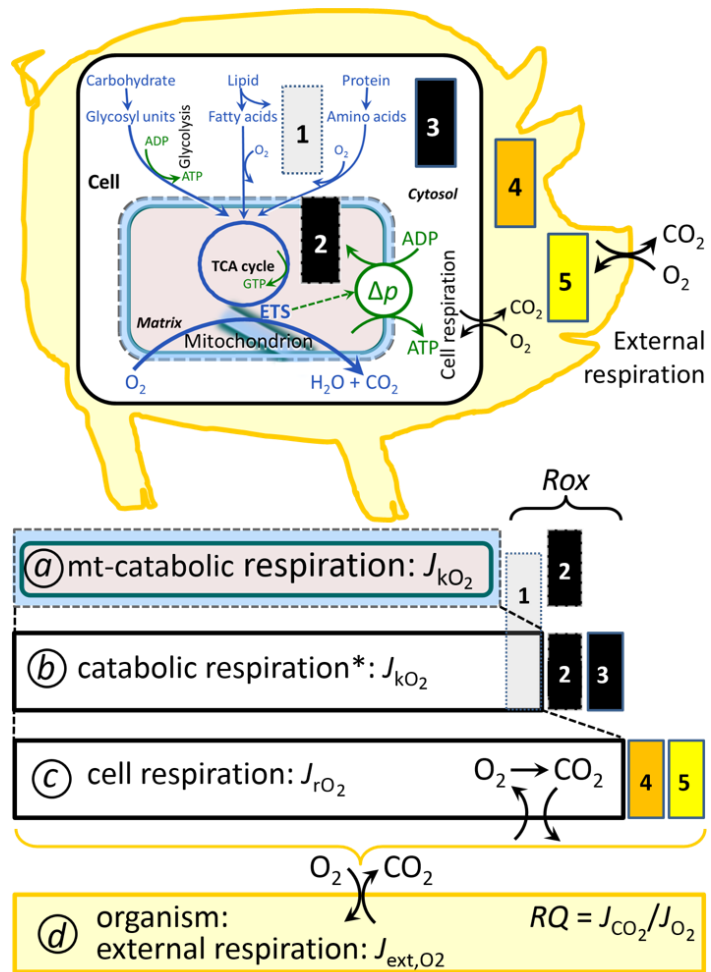
4. Mitochondrial coupling states are defined according to the control of respiratory oxygen flux by the protonmotive force. Capacities of oxidative phosphorylation and electron transfer are measured at kinetically saturating concentrations of fuel substrates, ADP and inorganic phosphate, and O_2, or at optimal uncoupler concentrations, respectively, in the absence of Complex IV inhibitors such as NO, CO, or H_2S. Respiratory capacity is a measure of the upper bound of the rate of respiration, depends on the substrate type undergoing oxidation, and provides reference values for the diagnosis of health and disease, and for evaluation of the effects of **E**volutionary background, **A**ge, **G**ender and sex, **L**ifestyle and **E**nvironment (EAGLE).

5. Incomplete tightness of coupling, *i.e.*, some degree of uncoupling relative to the substrate-dependent coupling stoichiometry, is a characteristic of energy-transformations across membranes. Uncoupling is caused by a variety of physiological, pathological, toxicological, pharmacological and environmental conditions that exert an influence not only on the proton leak and cation cycling, but also on proton slip within the proton pumps and the structural integrity of the mitochondria. A more loosely coupled state is induced by stimulation of mitochondrial superoxide formation and the bypass of proton pumps. In addition, uncoupling by application of protonophores represents an experimental intervention for the transition from a well-coupled to the noncoupled state of mitochondrial respiration.

6. Respiratory oxygen consumption rates have to be carefully normalized to enable meta-analytic studies beyond the specific question of a particular experiment. Therefore, all raw data should be published in a supplemental table or open access data repository. Normalization of rates for the volume of the experimental chamber (the measuring system) is distinguished from normalization for: (*1*) the volume or mass of the experimental sample; (*2*) the number of objects (cells, organisms); and (*3*) the concentration of mitochondrial markers in the chamber.

7. The consistent use of terms and symbols will facilitate transdisciplinary communication and support further developments of a database on bioenergetics and mitochondrial physiology. The present considerations are focused on studies with mitochondrial preparations. These will be extended in a series of reports on pathway control of mitochondrial respiration, the protonmotive force, respiratory states in intact cells, and harmonization of experimental procedures.

Box 1: In brief – Mitochondria and Bioblasts

'*For the physiologist, mitochondria afforded the first opportunity for an experimental approach to structure-function relationships, in particular those involved in active transport, vectorial metabolism, and metabolic control mechanisms on a subcellular level*' (Ernster and Schatz 1981).

Mitochondria are the oxygen-consuming electrochemical generators evolved from endosymbiotic bacteria (Margulis 1970; Lane 2005). They were described by Richard Altmann (1894) as 'bioblasts', which include not only the mitochondria as presently defined, but also symbiotic and free-living bacteria. The word 'mitochondria' (Greek mitos: thread; chondros: granule) was introduced by Carl Benda (1898).

Mitochondria form dynamic networks within eukaryotic cells and are morphologically enclosed by a double membrane. The mitochondrial inner membrane (mtIM) shows dynamic tubular to disk-shaped cristae that separate the mitochondrial matrix, *i.e.*, the negatively charged internal mitochondrial compartment, from the intermembrane space; the latter being enclosed by the mitochondrial outer membrane (mtOM) and positively charged with respect to the

259 matrix. The mtIM contains the non-bilayer phospholipid cardiolipin, which is not present in
260 any other eukaryotic cellular membrane. Cardiolipin stabilizes and promotes the formation of
261 respiratory supercomplexes (SC $I_nIII_nIV_n$), which are supramolecular assemblies based upon
262 specific, though dynamic interactions between individual respiratory complexes (Greggio *et al.*
263 2017; Lenaz *et al.* 2017). Membrane fluidity exerts an influence on functional properties of
264 proteins incorporated in the membranes (Waczulikova *et al.* 2007). In addition to mitochondrial
265 movement along microtubules, mitochondrial morphology can change in response to energy
266 requirements of the cell via processes known as fusion and fission, through which mitochondria
267 communicate within a network (Chan 2006). Intracellular stress factors may cause shrinking or
268 swelling of the mitochondrial matrix, that can ultimately result in permeability transition.

269 Mitochondria are the structural and functional elements of cell respiration. Mitochondrial
270 respiration is the reduction of molecular oxygen by electron transfer coupled to electrochemical
271 proton translocation across the mtIM. In the process of oxidative phosphorylation (OXPHOS),
272 the catabolic reaction of oxygen consumption is electrochemically coupled to the
273 transformation of energy in the form of adenosine triphosphate (ATP; Mitchell 1961, 2011).
274 Mitochondria are the powerhouses of the cell which contain the machinery of the OXPHOS-
275 pathways, including transmembrane respiratory complexes (proton pumps with FMN, Fe-S and
276 cytochrome *b*, *c*, *aa₃* redox systems); alternative dehydrogenases and oxidases; the coenzyme
277 ubiquinone (Q); F-ATPase or ATP synthase; the enzymes of the tricarboxylic acid cycle, fatty
278 acid and amino acid oxidation; transporters of ions, metabolites and co-factors; iron/sulphur
279 cluster synthesis; and mitochondrial kinases related to energy transfer pathways. The
280 mitochondrial proteome comprises over 1,200 proteins (Calvo *et al.* 2015; 2017), mostly
281 encoded by nuclear DNA (nDNA), with a variety of functions, many of which are relatively
282 well known (*e.g.,* proteins regulating mitochondrial biogenesis or apoptosis), while others are
283 still under investigation, or need to be identified (*e.g.,* alanine transporter). Only lately it is
284 possible to use the mammalian mitochondrial proteome to discover and characterize the genetic
285 basis of mitochondrial diseases (Williams *et al.* 2016; Palmfeldt and Bross 2017).

286 There is a constant crosstalk between mitochondria and the other cellular components.
287 The crosstalk between mitochondria and endoplasmic reticulum is involved in the regulation of
288 calcium homeostasis, cell division, autophagy, differentiation, and anti-viral signaling (Murley
289 and Nunnari 2016). Mitochondria contribute to the formation of peroxisomes, which are hybrids
290 of mitochondrial and ER-derived precursors (Sugiura *et al.* 2017). Cellular mitochondrial
291 homeostasis (mitostasis) is maintained through regulation at both the transcriptional and post-
292 translational level. Cell signalling modules contribute to homeostatic regulation throughout the
293 cell cycle or even cell death by activating proteostatic modules (*e.g.*, the ubiquitin-proteasome
294 and autophagy-lysosome/vacuole pathways; specific proteases like N) and genome stability
295 modules in response to varying energy demands and stress cues (Quiros *et al.* 2016).
296 Acetylation is a post-translational modification capable of influencing the bioenergetic
297 response, with clinically significant implications for health and disease (Carrico *et al.* 2018).
298 Mitochondria can traverse cell boundaries in a process known as horizontal mitochondrial
299 transfer (Torralba *et al.* 2016).

300 Mitochondria typically maintain several copies of their own circular genome known as
301 mitochondrial DNA (mtDNA; hundred to thousands per cell; Cummins 1998), which is
302 maternally inherited. Biparental mitochondrial inheritance is documented in mammals, birds,
303 fish, reptiles and invertebrate groups, and is even the norm in some bivalve taxonomic groups
304 (Breton *et al.* 2007; White *et al.* 2008). The mitochondrial genome of the angiosperm *Amborella*
305 contains a record of six mitochondrial genome equivalents aquired by horizontal transfer of
306 entire genomes, two from angiosperms, three from algae and one from mosses (Rice *et al.*
307 2016). Hovever, some organisms such as *Cryptosporidium* species have morphologically and
308 functionally reduced mitochondria without DNA (Liu *et al.* 2016). In vertebrates but not all
309 invertebrates, mtDNA is compact (16.5 kB in humans) and encodes 13 protein subunits of the

transmembrane respiratory Complexes CI, CIII, CIV and F-ATPase, 22 tRNAs, and two RNAs. Additional gene content has been suggested to include microRNAs, piRNA, smithRNAs, repeat associated RNA, and even additional proteins (Duarte *et al.* 2014; Lee *et al.* 2015; Cobb *et al.* 2016). The mitochondrial genome requires nuclear-encoded mitochondrially targeted proteins for its maintenance and expression (Rackham *et al.* 2012). Both genomes encode peptides of the membrane spanning redox pumps (CI, CIII and CIV) and F-ATPase, leading to strong constraints in the coevolution of both genomes (Blier *et al.* 2001).

Mitochondrial dysfunction is associated with a wide variety of genetic and degenerative diseases. Robust mitochondrial function is supported by physical exercise and caloric balance, and is central for sustained metabolic health throughout life. Therefore, a more consistent presentation of mitochondrial physiology will improve our understanding of the etiology of disease, the diagnostic repertoire of mitochondrial medicine, with a focus on protective medicine, lifestyle and healthy aging.

Abbreviation: mt, as generally used in mtDNA. Mitochondrion is singular and mitochondria is plural.

1. Introduction

Mitochondria are the powerhouses of the cell with numerous physiological, molecular, and genetic functions (**Box 1**). Every study of mitochondrial health and disease is faced with **E**volution, **A**ge, **G**ender and sex, **L**ifestyle, and **E**nvironment (EAGLE) as essential background conditions intrinsic to the individual person or cohort, species, tissue and to some extent even cell line. As a large and coordinated group of laboratories and researchers, the mission of the global MitoEAGLE Network is to generate the necessary scale, type, and quality of consistent data sets and conditions to address this intrinsic complexity. Harmonization of experimental protocols and implementation of a quality control and data management system are required to interrelate results gathered across a spectrum of studies and to generate a rigorously monitored database focused on mitochondrial respiratory function. In this way, researchers from a variety of disciplines can compare their findings using clearly defined and accepted international standards.

Reliability and comparability of quantitative results depend on the accuracy of measurements under strictly-defined conditions. A conceptual framework is required to warrant meaningful interpretation and comparability of experimental outcomes carried out by research groups at different institutes. With an emphasis on quality of research, collected data can be useful far beyond the specific question of a particular experiment. Standardization and homogenization of terminology, methodology, and data sets could lead to the development of open-access databases such as those that have been developed for National Institutes of Health sponsored research in genetics, proteomics, and metabolomics. Enabling meta-analytic studies is the most economic way of providing robust answers to biological questions (Cooper *et al.* 2009). Vague or ambiguous jargon can lead to confusion and may relegate valuable signals to wasteful noise. For this reason, measured values must be expressed in standard units for each parameter used to define mitochondrial respiratory function. Harmonization of nomenclature and definition of technical terms are essential to improve the awareness of the intricate meaning of current and past scientific vocabulary, for documentation and integration into databases in general, and quantitative modelling in particular (Beard 2005). The focus on coupling states and fluxes through metabolic pathways of aerobic energy transformation in mitochondrial preparations is a first step in the attempt to generate a conceptually-oriented nomenclature in bioenergetics and mitochondrial physiology. Coupling states of intact cells, the protonmotive force, and respiratory control by fuel substrates and specific inhibitors of respiratory enzymes will be reviewed in subsequent communications.

2. Oxidative phosphorylation and coupling states in mitochondrial preparations

'Every professional group develops its own technical jargon for talking about matters of critical concern ... People who know a word can share that idea with other members of their group, and a shared vocabulary is part of the glue that holds people together and allows them to create a shared culture' (Miller 1991).

Mitochondrial preparations are defined as either isolated mitochondria, or tissue and cellular preparations in which the barrier function of the plasma membrane is disrupted. Since this entails the loss of cell viability, mitochondrial preparations are not studied *in vivo*. In contrast to isolated mitochondria and tissue homogenate preparations, mitochondria in permeabilized tissues and cells are *in situ* relative to the plasma membrane. The plasma membrane separates the intracellular compartment including the cytosol, nucleus, and organelles from the extracellular environment. The plasma membrane consists of a lipid bilayer with embedded proteins and attached organic molecules that collectively control the selective permeability of ions, organic molecules, and particles across the cell boundary. The intact plasma membrane prevents the passage of many water-soluble mitochondrial substrates and inorganic ions—such as succinate, adenosine diphosphate (ADP) and inorganic phosphate (P_i), that must be controlled at kinetically-saturating concentrations for the analysis of respiratory capacities. Despite of the activity of solute carriers, *e.g.*, SLC13A3 and SLC20A2, that transport these metabolites across the plasma membrane of various cell types, this limits the scope of investigations into mitochondrial respiratory function in intact cells (**Figure 2A**).

The cholesterol content of the plasma membrane is high compared to mitochondrial membranes. Therefore, mild detergents—such as digitonin and saponin—can be applied to selectively permeabilize the plasma membrane by interaction with cholesterol and allow free exchange of organic molecules and inorganic ions between the cytosol and the immediate cell environment, while maintaining the integrity and localization of organelles, cytoskeleton, and nucleus. Application of optimum concentrations of permeabilization agents (mild detergents or toxins) leads to washout of cytosolic marker enzymes—such as lactate dehydrogenase—and results in the complete loss of cell viability, tested by nuclear staining using membrane-impermeable dyes, while mitochondrial function remains intact, tested by cytochrome *c* addition, for example. Respiration of isolated mitochondria remains unaltered after the addition of low concentrations of digitonin or saponin, although care should be taken when isolating mitochondria from cancer cells since they have significantly higher contents of cholesterol in both membranes (Baggetto and Testa-Perussini, 1990). In addition to mechanical cell disruption during homogenization of tissue, permeabilization agents may be applied to ensure permeabilization of all cells in tissue homogenates. Suspensions of cells permeabilized in the respiration chamber and crude tissue homogenates contain all components of the cell at highly dilute concentrations. All mitochondria are retained in chemically-permeabilized mitochondrial preparations and crude tissue homogenates. In the preparation of isolated mitochondria, however, the mitochondria are separated from other cell fractions and purified by differential centrifugation, entailing the loss of a fraction of the total mitochondrial content. Typical mitochondrial recovery ranges from 30% to 80%. Using Percoll or sucrose density gradients to maximize the purity of isolated mitochondria may compromise the mitochondrial yield or structural and functional integrity. Therefore, protocols to isolate mitochondria need to be optimized according to each study. The term mitochondrial preparation does neither include further fractionation of mitochondrial components, nor submitochondrial particles.

2.1. Respiratory control and coupling

Respiratory coupling control states are established in studies of mitochondrial preparations to obtain reference values for various output variables (**Table 1**). Physiological

412   conditions *in vivo* deviate from these experimentally obtained states. Since kinetically-
413   saturating concentrations, *e.g.,* of ADP or oxygen (O_2; dioxygen), may not apply to
414   physiological intracellular conditions, relevant information is obtained in studies of kinetic
415   responses to variations in [ADP] or [O_2] in the range between kinetically-saturating
416   concentrations and anoxia (Gnaiger 2001).
417   **The steady-state:** Mitochondria represent a thermodynamically open system in non-
418   equilibrium states of biochemical energy transformation. State variables (protonmotive force;
419   redox states) and metabolic *rates* (fluxes) are measured in defined mitochondrial respiratory
420   *states*. Steady-states can be obtained only in open systems, in which changes by *internal*
421   transformations, *e.g.*, O_2 consumption, are instantaneously compensated for by *external* fluxes,
422   *e.g.*, O_2 supply, preventing a change of O_2 concentration in the system (Gnaiger 1993b).
423   Mitochondrial respiratory states monitored in closed systems satisfy the criteria of pseudo-
424   steady states for limited periods of time, when changes in the system (concentrations of O_2, fuel
425   substrates, ADP, P_i, H^+) do not exert significant effects on metabolic fluxes (respiration,
426   phosphorylation). Such pseudo-steady states require respiratory media with sufficient buffering
427   capacity and substrates maintained at kinetically-saturating concentrations, and thus depend on
428   the kinetics of the processes under investigation.
429   **Specification of biochemical dose:** Substrates, uncouplers, inhibitors, and other
430   chemical reagents are titrated to dissect mitochondrial function. Nominal concentrations of
431   these substances are usually reported as initial amount of substance concentration [$mol·L^{-1}$] in
432   the incubation medium. When aiming at the measurement of kinetically saturated processes—
433   such as OXPHOS-capacities, the concentrations for substrates can be chosen according to the
434   apparent equilibrium constant, K_m'. In the case of hyperbolic kinetics, only 80% of maximum
435   respiratory capacity is obtained at a substrate concentration of four times the K_m', whereas
436   substrate concentrations of 5, 9, 19 and 49 times the K_m' are theoretically required for reaching
437   83%, 90%, 95% or 98% of the maximal rate (Gnaiger 2001). Other reagents are chosen to
438   inhibit or alter some processes. The amount of these chemicals in an experimental incubation
439   is selected to maximize effect, avoiding unacceptable off-target consequences that would
440   adversely affect the data being sought. Specifying the amount of substance in an incubation as
441   nominal concentration in the aqueous incubation medium can be ambiguous (Doskey *et al*.
442   2015), particularly for lipophilic substances (oligomycin, uncouplers, permeabilization agents)
443   or cations (TPP^+; fluorescent dyes such as safranin, TMRM; Chowdhury *et al.* 2015), which
444   accumulate in biological membranes or in the mitochondrial matrix. For example, a dose of
445   digitonin of 8 $fmol·cell^{-1}$ (10 $pg·cell^{-1}$; 10 $µg·10^{-6}$ cells) is optimal for permeabilization of
446   endothelial cells, and the concentration in the incubation medium has to be adjusted according
447   to the cell density applied (Doerrier *et al.* 2018).
448   Generally, dose/exposure can be specified per unit of biological sample, *i.e.*, (nominal
449   moles of xenobiotic)/(number of cells) [$mol·cell^{-1}$] or, as appropriate, per mass of biological
450   sample [$mol·kg^{-1}$]. This approach to specification of dose/exposure provides a scalable
451   parameter that can be used to design experiments, help interpret a wide variety of experimental
452   results, and provide absolute information that allows researchers worldwide to make the most
453   use of published data (Doskey *et al.* 2015).
454   **Phosphorylation, P», and P»/O_2 ratio:** *Phosphorylation* in the context of OXPHOS is
455   defined as phosphorylation of ADP by P_i to form ATP. On the other hand, the term
456   phosphorylation is used generally in many contexts, *e.g.,* protein phosphorylation. This justifies
457   consideration of a symbol more discriminating and specific than P as used in the P/O ratio
458   (phosphate to atomic oxygen ratio), where P indicates phosphorylation of ADP to ATP or GDP
459   to GTP (**Figure 2**). We propose the symbol P» for the endergonic (uphill) direction of
460   phosphorylation ADP→ATP, and likewise the symbol P« for the corresponding exergonic
461   (downhill) hydrolysis ATP→ADP (**Figure 3**). P» refers mainly to electrontransfer
462   phosphorylation but may also involve substrate-level phosphorylation as part of the

463   tricarboxylic acid (TCA) cycle (succinyl-CoA ligase; phosphoglycerate kinase) and
464   phosphorylation of ADP catalyzed by pyruvate kinase, and of GDP phosphorylated by
465   phosphoenolpyruvate carboxykinase. Transphosphorylation is performed by adenylate kinase,
466   creatine kinase (mtCK), hexokinase and nucleoside diphosphate kinase. In isolated mammalian
467   mitochondria, ATP production catalyzed by adenylate kinase ($2\ ADP \leftrightarrow ATP + AMP$) proceeds
468   without fuel substrates in the presence of ADP (Komlódi and Tretter 2017). Kinase cycles are
469   involved in intracellular energy transfer and signal transduction for regulation of energy flux.

470
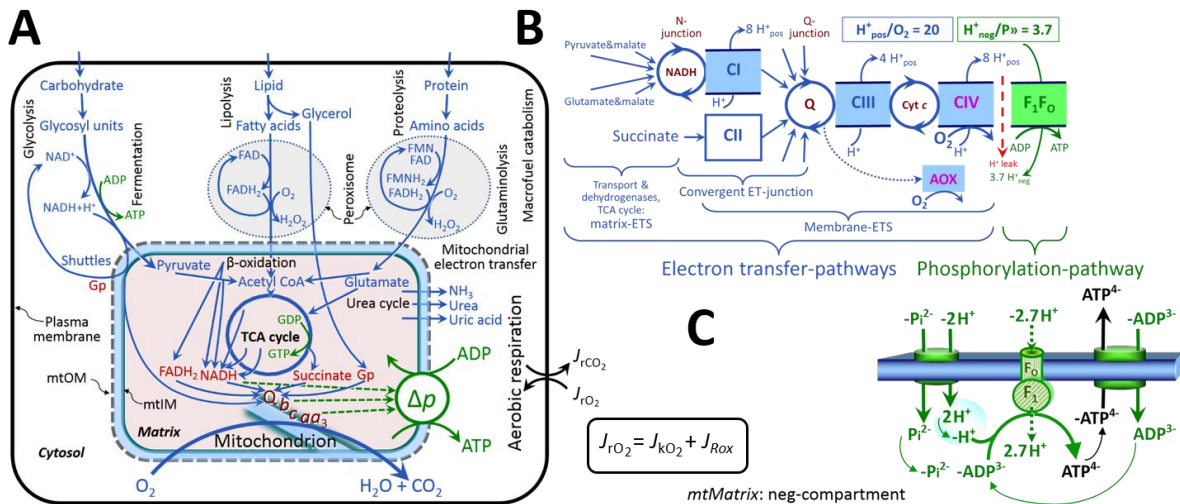
471
472   **Figure 2. Cell respiration and oxidative phosphorylation (OXPHOS)**
473   Mitochondrial respiration is the oxidation of fuel substrates (electron donors) with electron
474   transfer to O_2 as the electron acceptor. For explanation of symbols see also **Figure 1**.
475   **(A)** Respiration of intact cells: Extra-mitochondrial catabolism of macrofuels or uptake of small
476   molecules by the cell provides the *mitochondrial* fuel substrates. Many fuel substrates are
477   catabolized to acetyl-CoA or to glutamate, and further electron transfer reduces nicotinamide
478   adenine dinucleotide to NADH or flavin adenine dinucleotide to $FADH_2$. In respiration,
479   electron transfer is coupled to the phosphorylation of ADP to ATP, with energy transformation
480   mediated by the protonmotive force, Δp. Anabolic reactions are linked to catabolism, both by
481   ATP as the intermediary energy currency and by small organic precursor molecules as building
482   blocks for biosynthesis (not shown). Glycolysis involves substrate-level phosphorylation of
483   ADP to ATP in fermentation without utilization of O_2. In contrast, extra-mitochondrial
484   oxidation of fatty acids and amino acids proceeds partially in peroxisomes without coupling to
485   ATP production: acyl-CoA oxidase catalyzes the oxidation of $FADH_2$ with electron transfer to
486   O_2; amino acid oxidases oxidize flavin mononucleotide $FMNH_2$ or $FADH_2$. Coenzyme Q, Q,
487   and the cytochromes *b*, *c*, and *aa₃* are redox systems of the mitochondrial inner membrane,
488   mtIM. Dashed arrows indicate the connection between the redox proton pumps (respiratory
489   Complexes CI, CIII and CIV) and the transmembrane Δp. Mitochondrial outer membrane,
490   mtOM; glycerol-3-phosphate, Gp; tricarboxylic acid cycle, TCA cycle.
491   **(B)** Respiration in mitochondrial preparations: The mitochondrial electron transfer system
492   (ETS) is (*1*) fuelled by diffusion and transport of substrates across the mitochondrial outer and
493   inner membrane, and in addition consists of the (*2*) matrix-ETS, and (*3*) membrane-ETS.
494   Upstream sections of ET-pathways converge at the N-junction. NADH mainly generated in the
495   TCA cycle is oxidized by CI and electron entry into the Q-junction. Similarly, succinate is
496   formed in the TCA cycle and oxidized by CII to fumarate. CII is part of both the TCA cycle
497   and the ETS, and reduces FAD to $FADH_2$ with further reduction of ubiquinone to ubiquinol
498   downstream of the TCA cycle in the Q-junction. Thus $FADH_2$ is not a substrate but is the
499   product of CII, in contrast to erroneous metabolic maps shown in many textbooks and
500   publications. Unspecified arrows converging at the Q-junction indicate additional ET-sections

with electron entry into Q through electron transferring flavoprotein, glycerophosphate dehydrogenase, dihydro-orotate dehydrogenase, proline dehydrogenase, choline dehydrogenase, and sulfide-ubiquinone oxidoreductase. The dotted arrow indicates the branched pathway of oxygen consumption by alternative quinol oxidase (AOX). ET-pathways are coupled to the phosphorylation-pathway. The H^+_{pos}/O_2 ratio is the outward proton flux from the matrix space to the positively (pos) charged vesicular compartment, divided by catabolic O_2 flux in the NADH-pathway. The $H^+_{neg}/P»$ ratio is the inward proton flux from the inter-membrane space to the negatively (neg) charged matrix space, divided by the flux of phosphorylation of ADP to ATP. These stoichiometries are not fixed due to ion leaks and proton slip.

(C) Chemiosmotic phosphorylation-pathway catalyzed by the proton pump F_1F_O-ATPase (F-ATPase, ATP synthase), adenine nucleotide translocase, and inorganic phosphate transporter. The $H^+_{neg}/P»$ stoichiometry is the sum of the coupling stoichiometry in the F-ATPase reaction (-2.7 H^+_{pos} from the positive intermembrane space, 2.7 H^+_{neg} to the matrix, *i.e.*, the negative compartment) and the proton balance in the translocation of ADP^{3-}, ATP^{4-} and P_i^{2-}. Modified from (B) Lemieux *et al.* (2017) and (C) Gnaiger (2014).

The $P»/O_2$ ratio ($P»/4\,e^-$) is two times the 'P/O' ratio ($P»/2\,e^-$) of classical bioenergetics. $P»/O_2$ is a generalized symbol, not specific for determination of P_i consumption (P_i/O_2 flux ratio), ADP depletion (ADP/O_2 flux ratio), or ATP production (ATP/O_2 flux ratio). The mechanistic $P»/O_2$ ratio—or $P»/O_2$ stoichiometry—is calculated from the proton–to–O_2 and proton–to–phosphorylation coupling stoichiometries (**Figure 2B**):

$$P»/O_2 \;=\; \frac{H^+_{pos}/O_2}{H^+_{neg}/P»} \tag{1}$$

The H^+_{pos}/O_2 *coupling stoichiometry* (referring to the full 4 electron reduction of O_2) depends on the relative involvement of the three coupling sites (respiratory Complexes I, III and IV; CI, CIII and CIV) in the catabolic ET-pathway from reduced fuel substrates (electron donors) to the reduction of O_2 (electron acceptor). This varies with: (*1*) a bypass of CI by single or multiple electron input into the Q-junction; and (*2*) a bypass of CIV by involvement of alternative oxidases, AOX, which are not expressed in mammalian mitochondria.

H^+_{pos}/O_2 is 12 in the ET-pathways involving CIII and CIV as proton pumps, increasing to 20 for the NADH-pathway through CI (**Figure 2B**), but a general consensus on H^+_{pos}/O_2 stoichiometries remains to be reached (Hinkle 2005; Wikström and Hummer 2012; Sazanov 2015). The $H^+_{neg}/P»$ coupling stoichiometry (3.7; **Figure 2B**) is the sum of 2.7 H^+_{neg} required by the F-ATPase of vertebrate and most invertebrate species (Watt *et al.* 2010) and the proton balance in the translocation of ADP, ATP and P_i (**Figure 2C**). Taken together, the mechanistic $P»/O_2$ ratio is calculated at 5.4 and 3.3 for NADH- and succinate-linked respiration, respectively (Eq. 1). The corresponding classical $P»/O$ ratios (referring to the 2 electron reduction of 0.5 O_2) are 2.7 and 1.6 (Watt *et al.* 2010), in agreement with the measured $P»/O$ ratio for succinate of 1.58 ± 0.02 (Gnaiger *et al.* 2000).

The effective $P»/O_2$ flux ratio ($Y_{P»/O_2} = J_{P»}/J_{kO_2}$; **Figure 3**) is diminished relative to the mechanistic $P»/O_2$ ratio by intrinsic and extrinsic uncoupling and dyscoupling (**Figure 4**). Such generalized uncoupling is different from switching to mitochondrial pathways that involve fewer than three proton pumps ('coupling sites': Complexes CI, CIII and CIV), bypassing CI through multiple electron entries into the Q-junction, or CIII and CIV through AOX (**Figure 2B**). Reprogramming of mitochondrial pathways leading to different types of substrates being oxidized may be considered as a switch of gears (changing the stoichiometry by altering the substrate that is oxidized) rather than uncoupling (loosening the tightness of coupling relative to a fixed stoichiometry). In addition, $Y_{P»/O_2}$ depends on several experimental conditions of flux control, increasing as a hyperbolic function of [ADP] to a maximum value (Gnaiger 2001).

Control and regulation: The terms metabolic *control* and *regulation* are frequently used synonymously, but are distinguished in metabolic control analysis: 'We could understand the regulation as the mechanism that occurs when a system maintains some variable constant over time, in spite of fluctuations in external conditions (homeostasis of the internal state). On the other hand, metabolic control is the power to change the state of the metabolism in response to an external signal' (Fell 1997). Respiratory control may be induced by experimental control signals that *exert* an influence on: (*1*) ATP demand and ADP phosphorylation-rate; (*2*) fuel substrate composition, pathway competition; (*3*) available amounts of substrates and O_2, *e.g.*, starvation and hypoxia; (*4*) the protonmotive force, redox states, flux–force relationships, coupling and efficiency; (*5*) Ca^{2+} and other ions including H^+; (*6*) inhibitors, *e.g.*, nitric oxide or intermediary metabolites such as oxaloacetate; (*7*) signalling pathways and regulatory proteins, *e.g.,* insulin resistance, transcription factor hypoxia inducible factor 1. *Mechanisms* of respiratory control and regulation include adjustments of: (*1*) enzyme activities by allosteric mechanisms and phosphorylation; (*2*) enzyme content, concentrations of cofactors and conserved moieties—such as adenylates, nicotinamide adenine dinucleotide [NAD^+/NADH], coenzyme Q, cytochrome *c*; (*3*) metabolic channeling by supercomplexes; and *(4)* mitochondrial density (enzyme concentrations and membrane area) and morphology (cristae folding, fission and fusion). Mitochondria are targeted directly by hormones, thereby affecting their energy metabolism (Lee *et al.* 2013; Gerö and Szabo 2016; Price and Dai 2016; Moreno *et al.* 2017). Evolutionary or acquired differences in the genetic and epigenetic basis of mitochondrial function (or dysfunction) between individuals; age; gender, biological sex, and hormone concentrations; life style including exercise and nutrition; and environmental issues including thermal, atmospheric, toxic and pharmacological factors, exert an influence on all control mechanisms listed above. For reviews, see Brown 1992; Gnaiger 1993a, 2009; 2014; Paradies *et al.* 2014; Morrow *et al.* 2017.
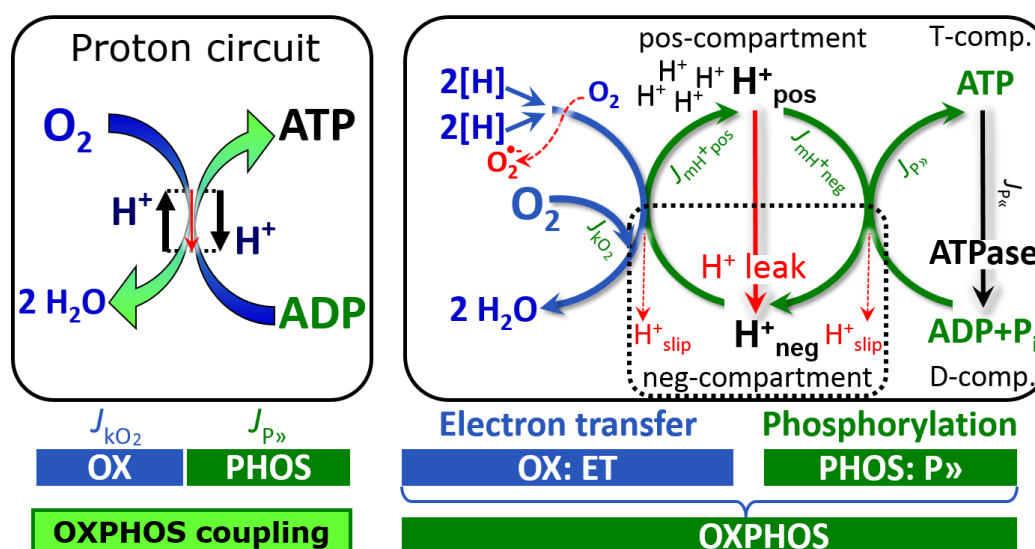
Figure 3. Coupling in oxidative phosphorylation (OXPHOS)
2[H] indicates the reduced hydrogen equivalents of fuel substrates of the catabolic reaction k with oxygen. O_2 flux, J_{kO_2}, through the catabolic ET-pathway, is coupled to flux through the phosphorylation-pathway of ADP to ATP, $J_{P»}$. The redox proton pumps of the ET-pathway drive proton flux into the positive (pos) compartment, J_{mH+pos}, generating the output protonmotive force (motive, subscript m). F-ATPase is coupled to inward proton current into the negative (neg) compartment, J_{mH+neg}, to phosphorylate ADP to ATP. The system is defined by the boundaries (full black line) and is not a black box, but is analysed as a compartmental system. The negative compartment (neg–compartment, enclosed by the dotted line) is the matrix space, separated by the mtIM from the positive compartment (pos–compartment).

588 ADP+P_i and ATP are the substrate- and product–compartments (scalar ADP and ATP
589 compartments, D–comp. and T–comp.), respectively. At steady-state proton turnover, $J_{\infty H+}$, and
590 ATP turnover, $J_{\infty P}$, maintain concentrations constant, when $J_{mH+\infty} = J_{mH+pos} = J_{mH+neg}$, and $J_{P\infty}$
591 $= J_{P\gg} = J_{P\ll}$. Modified from Gnaiger (2014).

593 **Respiratory control and response:** Lack of control by a metabolic pathway, *e.g.,*
594 phosphorylation-pathway, means that there will be no response to a variable activating it, *e.g.,*
595 [ADP]. The reverse, however, is not true as the absence of a response to [ADP] does not exclude
596 the phosphorylation-pathway from having some degree of control. The degree of control of a
597 component of the OXPHOS-pathway on an output variable—such as O_2 flux, will in general
598 be different from the degree of control on other outputs—such as phosphorylation-flux or
599 proton leak flux. Therefore, it is necessary to be specific as to which input and output are under
600 consideration (Fell 1997).
601 **Respiratory coupling control and ET-pathway control:** Respiratory control refers to
602 the ability of mitochondria to adjust O_2 flux in response to external control signals by engaging
603 various mechanisms of control and regulation. Respiratory control is monitored in a
604 mitochondrial preparation under conditions defined as respiratory states, preferentially under
605 near-physiological conditions of pH, temperature and medium ionic composition, to generate
606 data of higher biological relevance. When phosphorylation of ADP to ATP is stimulated or
607 depressed, an increase or decrease is observed in electron transfer measured as O_2 flux in
608 respiratory coupling states of intact mitochondria ('controlled states' in the classical
609 terminology of bioenergetics). Alternatively, coupling of electron transfer with phosphorylation
610 is disengaged by uncouplers. These protonophores are weak lipid-soluble acids which disrupt
611 the barrier function of the mtIM and thus shortcircuit the protonmotive system, functioning like
612 a clutch in a mechanical system. The corresponding coupling control state is characterized by
613 a high O_2 flux without control by P» (noncoupled or 'uncontrolled state').
614 ET-pathway control states are obtained in mitochondrial preparations by depletion of
615 endogenous substrates and addition to the mitochondrial respiration medium of fuel substrates
616 (**Figure 2**; 2[H] in **Figure 3**) and specific inhibitors, activating selected mitochondrial catabolic
617 pathways, k, of electron transfer from the oxidation of fuel substrates to reduction of O_2 (**Figure**
618 **2A**). Coupling control states and pathway control states are complementary, since
619 mitochondrial preparations depend on an exogenous supply of pathway-specific fuel substrates
620 and oxygen (Gnaiger 2014).
621 **Coupling:** In mitochondrial electron transfer, vectorial transmembrane proton flux is
622 coupled through the redox proton pumps CI, CIII and CIV to the catabolic flux of scalar
623 reactions, collectively measured as O_2 flux (**Figure 3**). Thus mitochondria are elements of
624 energy transformation. Energy is a conserved quantity and cannot be lost or produced in any
625 internal process (First Law of thermodynamics). Open and closed systems can gain or lose
626 energy only by external fluxes—by exchange with the environment. Therefore, energy can
627 neither be produced by mitochondria, nor is there any internal process without energy
628 conservation. Exergy or Gibbs energy ('free energy') is the part of energy that can potentially
629 be transformed into work under conditions of constant volume and pressure. *Coupling* is the
630 interaction of an exergonic process (spontaneous, negative exergy change) with an endergonic
631 process (positive exergy change) in energy transformations which conserve part of the exergy
632 that would be irreversibly lost or dissipated in an uncoupled process.
633 **Uncoupling:** Uncoupling of mitochondrial respiration is a general term comprising
634 diverse mechanisms:
635 1. Proton leak across the mtIM from the pos– to the neg–compartment (H^+ leak-
636 uncoupled; **Figure 4**).

2. Cycling of other cations, strongly stimulated by permeability transition; comparable to the use of protonophores, cation cycling is experimentally induced by valinomycin in the presence of K^+;

3. Decoupling by proton slip in the redox proton pumps when protons are effectively not pumped (CI, CIII and CIV) or are not driving phosphorylation (F-ATPase);

4. Loss of vesicular (compartmental) integrity when electron transfer is acoupled;

5. Electron leak in the loosely coupled univalent reduction of O_2 to superoxide ($O_2^{\bullet-}$; superoxide anion radical).

Differences of terms—uncoupled *vs.* noncoupled—are easily overlooked, although they relate to different meanings of uncoupling (**Figure 4** and **Table 2**).
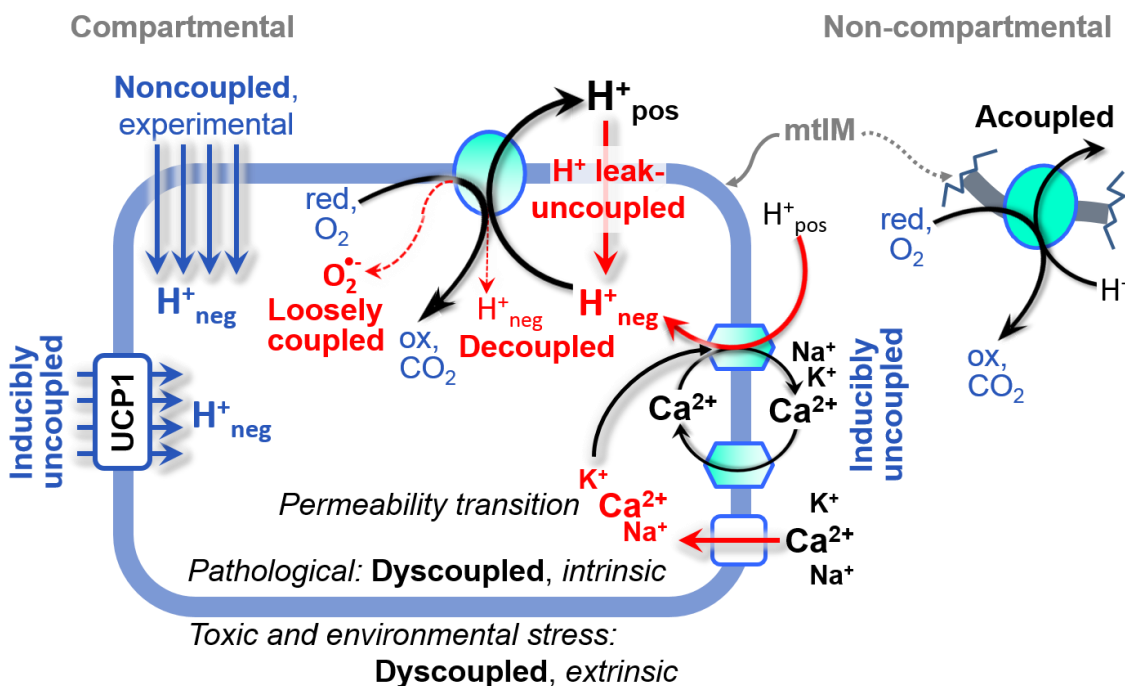
Figure 4. Mechanisms of respiratory uncoupling

An intact mitochondrial inner membrane, mtIM, is required for vectorial, compartmental coupling. 'Acoupled' respiration is the consequence of structural disruption with catalytic activity of non-compartmental mitochondrial fragments. Inducibly uncoupled (activation of UCP1) and experimentally noncoupled respiration (titration of protonophores) stimulate respiration to maximum O_2 flux. H^+ leak-uncoupled, decoupled, and loosely coupled respiration are components of intrinsic uncoupling. Pathological dysfunction may affect all types of uncoupling, including permeability transition, causing intrinsically dyscoupled respiration. Similarly, toxicological and environmental stress factors can cause extrinsically dyscoupled respiration.

2.2. Coupling states and respiratory rates

Respiratory capacities in coupling control states: To extend the classical nomenclature on mitochondrial coupling states (Section 2.3) by a concept-driven terminology that explicitly incorporates information on the meaning of respiratory states, the terminology must be general and not restricted to any particular experimental protocol or mitochondrial preparation (Gnaiger 2009). Concept-driven nomenclature aims at mapping the *meaning and concept behind* the words and acronyms onto the *forms* of words and acronyms (Miller 1991). The focus of

concept-driven nomenclature is primarily the conceptual 'why', along with clarification of the experimental 'how'. Respiratory capacities delineate, comparable to channel capacity in information theory (Schneider 2006), the upper bound of the rate of respiration measured in defined coupling control states and electron transfer-pathway (ET-pathway) states (**Figure 5**).

Figure 5. Four-compartment model of oxidative phosphorylation
Respiratory states (ET, OXPHOS, LEAK; **Table 1**) and corresponding rates (E, P, L) are connected by the protonmotive force, Δp. ET-capacity, E (1), is partitioned into (2) dissipative LEAK-respiration, L, when the Gibbs energy change of catabolic O$_2$ flux is irreversibly lost, (3) net OXPHOS-capacity, P-L, with partial conservation of the capacity to perform work, and (4) the excess capacity, E-P. Modified from Gnaiger (2014).
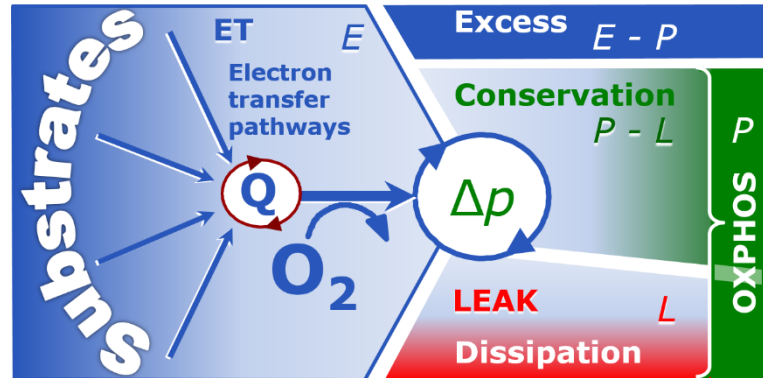
To provide a diagnostic reference for respiratory capacities of core energy metabolism, the capacity of *oxidative phosphorylation*, OXPHOS, is measured at kinetically-saturating concentrations of ADP and P$_i$. The *oxidative* ET-capacity reveals the limitation of OXPHOS-capacity mediated by the *phosphorylation*-pathway. The ET- and phosphorylation-pathways comprise coupled segments of the OXPHOS-system. ET-capacity is measured as noncoupled respiration by application of *external uncouplers*. The contribution of *intrinsically uncoupled* O$_2$ consumption is studied by preventing the stimulation of phosphorylation either in the absence of ADP or by inhibition of the phosphorylation-pathway. The corresponding states are collectively classified as LEAK-states, when O$_2$ consumption compensates mainly for ion leaks, including the proton leak. Defined coupling states are induced by: (1) adding cation chelators such as EGTA, binding free Ca^{2+} and thus limiting cation cycling; (2) adding ADP and P$_i$; (3) inhibiting the phosphorylation-pathway; and (4) uncoupler titrations, while maintaining a defined ET-pathway state with constant fuel substrates and inhibitors of specific branches of the ET-pathway (**Figure 5**).

The three coupling states, ET, LEAK and OXPHOS, are shown schematically with the corresponding respiratory rates, abbreviated as E, L and P, respectively (**Figure 5**). We distinguish metabolic *pathways* from metabolic *states* and the corresponding metabolic *rates*; for example: ET-pathways, ET-states, and ET-capacities, E, respectively (**Table 1**). The protonmotive force is *high* in the OXPHOS-state when it drives phosphorylation, *maximum* in the LEAK-state of coupled mitochondria, driven by LEAK-respiration at a minimum back-flux of cations to the matrix side, and *very low* in the ET-state when uncouplers short-circuit the proton cycle (**Table 1**).

LEAK-state (**Figure 6A**): The LEAK-state is defined as a state of mitochondrial respiration when O_2 flux mainly compensates for ion leaks in the absence of ATP synthesis, at kinetically-saturating concentrations of O_2, respiratory fuel substrates and P_i. LEAK-respiration is measured to obtain an estimate of *intrinsic uncoupling* without addition of an experimental uncoupler: (*1*) in the absence of adenylates, *i.e.*, AMP, ADP and ATP; (*2*) after depletion of ADP at a maximum ATP/ADP ratio; or (*3*) after inhibition of the phosphorylation-pathway by inhibitors of F-ATPase—such as oligomycin, or of adenine nucleotide translocase—such as carboxyatractyloside. Adjustment of the nominal concentration of these inhibitors to the density of biological sample applied can minimize or avoid inhibitory side-effects exerted on ET-capacity or even some dyscoupling.

Proton leak and uncoupled respiration: Proton leak is a leak current of protons. The intrinsic proton leak is the *uncoupled* process in which protons diffuse across the mtIM in the dissipative direction of the downhill protonmotive force without coupling to phosphorylation (**Figure 6A**). The proton leak flux depends non-linearly on the protonmotive force (Garlid *et al.* 1989; Divakaruni and Brand 2011), it is a temperature-dependent property of the mtIM and may be enhanced due to possible contaminations by free fatty acids. Inducible uncoupling mediated by uncoupling protein 1 (UCP1) is physiologically controlled, *e.g.*, in brown adipose tissue. UCP1 is a member of the mitochondrial carrier family that is involved in the translocation of protons across the mtIM (Klingenberg 2017).
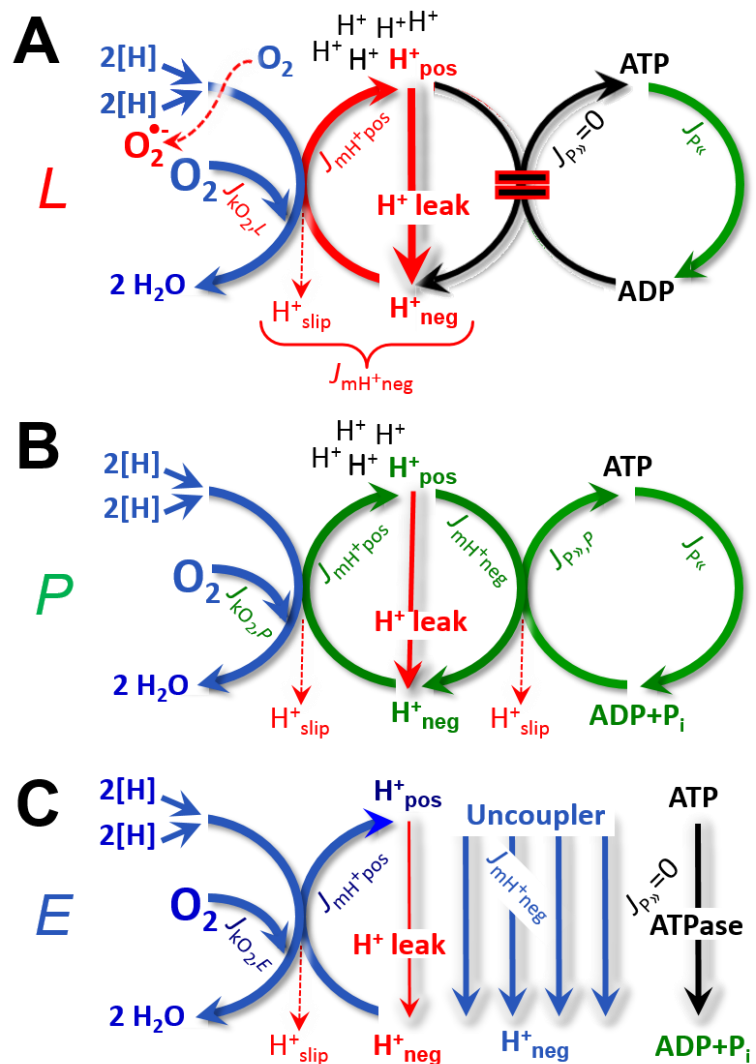
Figure 6. Respiratory coupling states

(A) LEAK-state and rate, L**:** Phosphorylation is arrested, $J_{P»} = 0$, and catabolic O_2 flux, $J_{kO_2,L}$, is controlled mainly by the proton leak, $J_{mH+neg,L}$, at maximum protonmotive force (**Figure 4**). Extramitochondrial ATP may be hydrolyzed by extramitochondrial ATPases, $J_{P«}$.

(B) OXPHOS-state and rate, P**:** Phosphorylation, $J_{P»}$, is stimulated by kinetically-saturating [ADP] and [P_i], and is supported by a high protonmotive force. O_2 flux, $J_{kO_2,P}$, is well-coupled at a $P»/O_2$ ratio of $J_{P»,P}/J_{O_2,P}$. Extramitochondrial ATPases may recycle ATP, $J_{P«}$.

(C) ET-state and rate, E**:** Noncoupled respiration, $J_{kO2,E}$, is maximum at optimum exogenous uncoupler concentration and phosphorylation is zero, $J_{P»} = 0$. The F-ATPase may hydrolyze extramitochondrial ATP. See also **Figure 3**.

764 Consequently, the short-circuit diminishes the protonmotive force and stimulates electron
765 transfer to O_2 and heat dissipation without phosphorylation of ADP.
766   **Cation cycling:** There can be other cation contributors to leak current including calcium
767 and probably magnesium. Calcium influx is balanced by mitochondrial Na^+/Ca^{2+} or H^+/Ca^{2+}
768 exchange, which is balanced by Na^+/H^+ or K^+/H^+ exchanges. This is another effective
769 uncoupling mechanism different from proton leak (**Table 2**).
770
771 **Table 1. Coupling states and residual oxygen consumption in mitochondrial**
772 **preparations in relation to respiration- and phosphorylation-flux, J_{kO_2} and $J_{P»}$,**
773 **and protonmotive force, Δp.** Coupling states are established at kinetically-
774 saturating concentrations of fuel substrates and O_2.

State	J_{kO_2}	$J_{P»}$	Δp	Inducing factors	Limiting factors
LEAK	L; low, cation leak-dependent respiration	0	max.	back-flux of cations including proton leak, proton slip	$J_{P»} = 0$: (*1*) without ADP, L_N; (*2*) max. ATP/ADP ratio, L_T; or (*3*) inhibition of the phosphorylation-pathway, L_{Omy}
OXPHOS	P; high, ADP-stimulated respiration	max.	high	kinetically-saturating [ADP] and [P_i]	$J_{P»}$ by phosphorylation-pathway; or J_{kO_2} by ET-capacity
ET	E; max., noncoupled respiration	0	low	optimal external uncoupler concentration for max. $J_{O_2,E}$	J_{kO_2} by ET-capacity
ROX	Rox; min., residual O_2 consumption	0	0	$J_{O_2,Rox}$ in non-ET-pathway oxidation reactions	inhibition of all ET-pathways; or absence of fuel substrates

775
776   **Proton slip and decoupled respiration:** Proton slip is the *decoupled* process in which
777 protons are only partially translocated by a redox proton pump of the ET-pathways and slip
778 back to the original vesicular compartment. The proton leak is the dominant contributor to the
779 overall leak current in mammalian mitochondria incubated under physiological conditions at
780 37 °C, whereas proton slip is increased at lower experimental temperature (Canton *et al.* 1995).
781 Proton slip can also happen in association with the F-ATPase, in which the proton slips downhill
782 across the pump to the matrix without contributing to ATP synthesis. In each case, proton slip
783 is a property of the proton pump and increases with the pump turnover rate.
784   **Electron leak and loosely coupled respiration**: Superoxide production by the ETS leads
785 to a bypass of redox proton pumps and correspondingly lower P»/O_2 ratio. This depends on the
786 actual site of electron leak and the scavenging of hydrogen peroxide by cytochrome *c*, whereby
787 electrons may re-enter the ETS with proton translocation by CIV.
788 **Loss of compartmental integrity and acoupled respiration:** Electron transfer and catabolic
789 O_2 flux proceed without compartmental proton translocation in disrupted mitochondrial
790 fragments. Such fragments form during mitochondrial isolation, and may not fully fuse to re-
791 establish structurally intact mitochondria. Loss of mtIM integrity, therefore, is the cause of
792 acoupled respiration, which is a nonvectorial dissipative process without control by the
793 protonmotive force.
794

Table 2. Terms on respiratory coupling and uncoupling.

Term		J_{kO_2}	P»/O₂	Note
acoupled			0	electron transfer in mitochondrial fragments without vectorial proton translocation (**Figure 4**)
	uncoupled	L	0	non-phosphorylating LEAK-respiration (**Figure 6A**)
	proton leak-uncoupled		0	component of L, H$^+$ diffusion across the mtIM (**Figure 4**)
	decoupled		0	component of L, proton slip (**Figure 4**)
	loosely coupled		0	component of L, lower coupling due to superoxide formation and bypass of proton pumps (**Figure 4**)
	dyscoupled		0	pathologically, toxicologically, environmentally increased uncoupling, mitochondrial dysfunction
	inducibly uncoupled		0	by UCP1 or cation (*e.g.,* Ca^{2+}) cycling (**Figure 4**)
noncoupled		E	0	non-phosphorylating respiration stimulated to maximum flux at optimum exogenous uncoupler concentration (**Figure 6C**)
well-coupled		P	high	phosphorylating respiration with an intrinsic LEAK component (**Figure 6B**)
fully coupled		$P - L$	max.	OXPHOS-capacity corrected for LEAK-respiration (**Figure 5**)

intrinsic, no protonophore added (brace spanning uncoupled through inducibly uncoupled rows)

Dyscoupled respiration: Mitochondrial injuries may lead to *dyscoupling* as a pathological or toxicological cause of *uncoupled* respiration. Dyscoupling may involve any type of uncoupling mechanism, *e.g.*, opening the permeability transition pore. Dyscoupled respiration is distinguished from the experimentally induced *noncoupled* respiration in the ET-state (**Table 2**).

OXPHOS-state (**Figure 6B**): The OXPHOS-state is defined as the respiratory state with kinetically-saturating concentrations of O₂, respiratory and phosphorylation substrates, and absence of exogenous uncoupler, which provides an estimate of the maximal respiratory capacity in the OXPHOS-state for any given ET-pathway state. Respiratory capacities at kinetically-saturating substrate concentrations provide reference values or upper limits of performance, aiming at the generation of data sets for comparative purposes. Physiological activities and effects of substrate kinetics can be evaluated relative to the OXPHOS-capacity.

As discussed previously, 0.2 mM ADP does not fully saturate flux in isolated mitochondria (Gnaiger 2001; Puchowicz *et al.* 2004); greater ADP concentration is required, particularly in permeabilized muscle fibres and cardiomyocytes, to overcome limitations by intracellular diffusion and by the reduced conductance of the mtOM (Jepihhina *et al.* 2011, Illaste *et al.* 2012, Simson *et al.* 2016), either through interaction with tubulin (Rostovtseva *et al.* 2008) or other intracellular structures (Birkedal *et al.* 2014). In addition, saturating ADP concentrations need to be evaluated under different experimental conditions such as temperature (Lemieux *et al.* 2017) and with different animal models (Blier and Guderley, 1993). In permeabilized muscle fibre bundles of high respiratory capacity, the apparent K_m for ADP increases up to 0.5 mM (Saks *et al.* 1998), consistent with experimental evidence that >90% saturation is reached only at >5 mM ADP (Pesta and Gnaiger 2012). Similar ADP concentrations are also required for accurate determination of OXPHOS-capacity in human

clinical cancer samples and permeabilized cells (Klepinin *et al.* 2016; Koit *et al.* 2017). Whereas 2.5 to 5 mM ADP is sufficient to obtain the actual OXPHOS-capacity in many types of permeabilized tissue and cell preparations, experimental validation is required in each specific case.

Electron transfer-state (**Figure 6C**): O_2 flux determined in the ET-state yields an estimate of ET-capacity. The ET-state is defined as the *noncoupled* state with kinetically-saturating concentrations of O_2, respiratory substrate and optimum *exogenous* uncoupler concentration for maximum O_2 flux. As a consequence of the nearly collapsed protonmotive force, the driving force is insufficient for phosphorylation, and $J_{P»} = 0$. The most frequently used uncouplers are carbonyl cyanide m-chloro phenyl hydrazone, carbonyl cyanide *p*-trifluoromethoxyphenylhydrazone or dinitrophinole (CCCP, FCCP, DNP). Stepwise titration of uncouplers stimulates respiration up to or above the level of O_2 consumption rates in the OXPHOS-state, but inhibition of respiration is observed above optimum uncoupler concentrations (Mitchell 2011). Data obtained with a single dose of uncoupler must be evaluated with caution, particularly when a fixed uncoupler concentration is used in studies exploring a treatment or disease that may alter the mitochondrial content or mitochondrial sensitivity to inhibition by uncouplers. The effect on ET-capacity of the reversed function of F-ATPase ($J_{P«}$; **Figure 6C**) can be evaluated in the presence and absence of extramitochondrial ATP.

ROX state and *Rox*: Besides the three fundamental coupling states of mitochondrial preparations, the state of residual O_2 consumption, ROX, is relevant to assess respiratory function (**Figure 1**). ROX is not a coupling state. The rate of residual oxygen consumption, *Rox*, is defined as O_2 consumption due to oxidative reactions measured after inhibition of ET—with rotenone, malonic acid and antimycin A. Cyanide and azide inhibit not only CIV but catalase and several peroxidases involved in *Rox*. However, high concentrations of antimycin A, but not rotenone or cyanide, inhibit peroxisomal acyl-CoA oxidase and D-amino acid oxidase (Vamecq *et al.* 1987). ROX represents a baseline that is used to correct respiration measured in defined coupling states. *Rox*-corrected *L*, *P* and *E* not only lower the values of total fluxes, but also changes the flux control ratios *L/P* and *L/E*. *Rox* is not necessarily equivalent to non-mitochondrial reduction of O_2, considering O_2-consuming reactions in mitochondria that are not related to ET—such as O_2 consumption in reactions catalyzed by monoamine oxidases (type A and B), monooxygenases (cytochrome P450 monooxygenases), dioxygenase (sulfur dioxygenase and trimethyllysine dioxygenase), and several hydoxylases. Even isolated mitochondrial fractions, especially those obtained from liver, may be contaminated by peroxisomes. This fact makes the exact determination of mitochondrial O_2 consumption and mitochondria-associated generation of reactive oxygen species complicated (Schönfeld *et al.* 2009; Speijer 2016; **Figure 2**). The dependence of ROX-linked O_2 consumption needs to be studied in detail together with non-ET enzyme activities, availability of specific substrates, O_2 concentration, and electron leakage leading to the formation of reactive oxygen species.

Quantitative relations: *E* may exceed or be equal to *P*. $E > P$ is observed in many types of mitochondria, varying between species, tissues and cell types (Gnaiger 2009). *E-P* is the excess ET-capacity pushing the phosphorylation-flux (**Figure 2C**) to the limit of its *capacity of utilizing* the protonmotive force. In addition, the magnitude of *E-P* depends on the tightness of respiratory coupling or degree of uncoupling, since an increase of *L* causes *P* to increase towards the limit of *E*. The *excess E-P* capacity, *E-P*, therefore, provides a sensitive diagnostic indicator of specific injuries of the phosphorylation-pathway, under conditions when *E* remains constant but *P* declines relative to controls (**Figure 5**). Substrate cocktails supporting simultaneous convergent electron transfer to the Q-junction for reconstitution of TCA cycle function establish pathway control states with high ET-capacity, and consequently increase the sensitivity of the *E-P* assay.

871   *E* cannot theoretically be lower than *P*. <mark>*E* < *P* must be discounted as an artefact</mark>, which
872 may be caused experimentally by: (*1*) loss of oxidative capacity during the time course of the
873 respirometric assay, since *E* is measured subsequently to *P*; (*2*) using insufficient uncoupler
874 concentrations; (*3*) using high uncoupler concentrations which inhibit ET (Gnaiger 2008); (*4*)
875 high oligomycin concentrations applied for measurement of *L* before titrations of uncoupler,
876 when oligomycin exerts an inhibitory effect on *E*. On the other hand, the excess ET-capacity is
877 overestimated if non-saturating [ADP] or [P$_i$] are used. See State 3 in the next section.
878   The net OXPHOS-capacity is calculated by subtracting *L* from *P* (**Figure 5**). The net
879 P»/O$_2$ equals P»/(*P-L*), wherein the dissipative LEAK component in the OXPHOS-state may
880 be overestimated. This can be avoided by measuring LEAK-respiration in a state when the
881 protonmotive force is adjusted to its slightly lower value in the OXPHOS-state—by titration of
882 an ET inhibitor (Divakaruni and Brand 2011). Any turnover-dependent components of proton
883 leak and slip, however, are underestimated under these conditions (Garlid *et al.* 1993). In
884 general, it is inappropriate to use the term *ATP production* or *ATP turnover* for the difference
885 of O$_2$ flux measured in the OXPHOS and LEAK states. *P-L* is the upper limit of OXPHOS-
886 capacity that is freely available for ATP production (corrected for LEAK-respiration) and is
887 fully coupled to phosphorylation with a maximum mechanistic stoichiometry (**Figure 5**).
888   The rates of LEAK respiration and OXPHOS capacity depend on (*1*) the tightness of
889 coupling under the influence of the respiratory uncoupling mechanisms (**Figure 4**), and (*2*) the
890 coupling stoichiometry, which varies as a function of the substrate type undergoing oxidation
891 in ET-pathways with either two or three coupling sites (**Figure 2B**). When cocktails with
892 NADH-linked substrates and succinate are used, the relative contribution of ET-pathways with
893 three or two coupling sites cannot be controlled experimentally, is difficult to determine, and
894 may shift in transitions between LEAK-, OXPHOS- and ET-states (Gnaiger 2014). Under these
895 experimental conditions, we cannot separate the tightness of coupling *versus* coupling
896 stoichiometry as the mechanisms of respiratory control in the shift of *L/P* ratios. The tightness
897 of coupling and fully coupled O$_2$ flux, *P-L* (**Table 2**), therefore, are obtained from
898 measurements of coupling control of LEAK respiration, OXPHOS- and ET-capacities in well
899 defined pathway states, using either pyruvate and malate as substrates or the classical succinate
900 and rotenone substrate-inhibitor combination (**Figure 2B**).

902 *2.3.* <mark>*Classical terminology for isolated mitochondria*</mark>
903   *'When a code is familiar enough, it ceases appearing like a code; one forgets that there*
904   *is a decoding mechanism. The message is identical with its meaning'* (Hofstadter 1979).

906   Chance and Williams (1955; 1956) introduced five classical states of mitochondrial
907 respiration and cytochrome redox states. **Table 3** shows a protocol with isolated mitochondria
908 in a closed respirometric chamber, defining a sequence of respiratory states. States and rates
909 are not specifically distinguished in this nomenclature.

911 **Table 3. Metabolic states of mitochondria (Chance and**
912 **Williams, 1956; Table V).**
913

State	[O$_2$]	ADP level	Substrate level	Respiration rate	Rate-limiting substance
1	>0	low	low	slow	ADP
2	>0	high	~0	slow	substrate
3	>0	high	high	fast	respiratory chain
4	>0	low	high	slow	ADP
5	0	high	high	0	oxygen

914

915   **State 1** is obtained after addition of isolated mitochondria to air-saturated
916 isoosmotic/isotonic respiration medium containing P_i, but no fuel substrates and no adenylates,
917 *i.e.*, AMP, ADP, ATP.
918   **State 2** is induced by addition of a 'high' concentration of ADP (typically 100 to 300
919 µM), which stimulates respiration transiently on the basis of endogenous fuel substrates and
920 phosphorylates only a small portion of the added ADP. State 2 is then obtained at a low
921 respiratory activity limited by exhausted endogenous fuel substrate availability (**Table 3**). If
922 addition of specific inhibitors of respiratory complexes—such as rotenone—does not cause a
923 further decline of O_2 flux, State 2 is equivalent to the ROX state (See below.). If inhibition is
924 observed, undefined endogenous fuel substrates are a confounding factor of pathway control,
925 contributing to the effect of subsequently externally added substrates and inhibitors. In contrast
926 to the original protocol, an alternative sequence of titration steps is frequently applied, in which
927 the alternative 'State 2' has an entirely different meaning, when this second state is induced by
928 addition of fuel substrate without ADP or ATP (LEAK-state; in contrast to State 2 defined in
929 **Table 1** as a ROX state). Some researchers have called this condition as "pseudostate 4"
930 because it has no significant concentrations of adenine nucleotides and hence it is not a near-
931 physiological condition, although it should be used for calculating the net OXPHOS-capacity,
932 *P-L*.
933   **State 3** is the state stimulated by addition of fuel substrates while the ADP concentration
934 is still high (**Table 3**) and supports coupled energy transformation through oxidative
935 phosphorylation. 'High ADP' is a concentration of ADP specifically selected to allow the
936 measurement of State 3 to State 4 transitions of isolated mitochondria in a closed respirometric
937 chamber. Repeated ADP titration re-establishes State 3 at 'high ADP'. Starting at O_2
938 concentrations near air-saturation (193 or 238 µM O_2 at 37 °C or 25 °C and sea level at 1 atm
939 or 101.32 kPa, and an oxygen solubility of respiration medium at 0.92 times that of pure water;
940 Forstner and Gnaiger 1983), the total ADP concentration added must be low enough (typically
941 100 to 300 µM) to allow phosphorylation to ATP at a coupled O_2 flux that does not lead to O_2
942 depletion during the transition to State 4. In contrast, kinetically-saturating ADP concentrations
943 usually are 10-fold higher than 'high ADP', *e.g.,* 2.5 mM in isolated mitochondria. The
944 abbreviation State 3u is occasionally used in bioenergetics, to indicate the state of respiration
945 after titration of an uncoupler, without sufficient emphasis on the fundamental difference
946 between OXPHOS-capacity (*well-coupled* with an *endogenous* uncoupled component) and ET-
947 capacity (*noncoupled*).
948   **State 4** is a LEAK-state that is obtained only if the mitochondrial preparation is intact
949 and well-coupled. Depletion of ADP by phosphorylation to ATP causes a decline of O_2 flux in
950 the transition from State 3 to State 4. Under the conditions of State 4, a maximum protonmotive
951 force and high ATP/ADP ratio are maintained. The gradual decline of $Y_{P»/O_2}$ towards
952 diminishing [ADP] at State 4 must be taken into account for calculation of P»/O_2 ratios (Gnaiger
953 2001). State 4 respiration, L_T (**Table 1**), reflects intrinsic proton leak and ATP hydrolysis
954 activity. O_2 flux in State 4 is an overestimation of LEAK-respiration if the contaminating ATP
955 hydrolysis activity recycles some ATP to ADP, $J_{P«}$, which stimulates respiration coupled to
956 phosphorylation, $J_{P»} > 0$. Some degree of mechanical disruption and loss of mitochondrial
957 integrity allows the exposed mitochondrial F-ATPases to hydrolyze the ATP synthesized by
958 the fraction of coupled mitochondria. This can be tested by inhibition of the phosphorylation-
959 pathway using oligomycin, ensuring that $J_{P»} = 0$ (State 4o). On the other hand, the state 4
960 respiration reached after exhaustion of added ADP is a more physiological condition (*i.e.*,
961 presence of ATP, ADP and even AMP). Sequential ADP titrations re-establish State 3, followed
962 by State 3 to State 4 transitions while sufficient O_2 is available. Anoxia may be reached,
963 however, before exhaustion of ADP (State 5).
964   **State 5** is the state after exhaustion of O_2 in a closed respirometric chamber. Diffusion of
965 O_2 from the surroundings into the aqueous solution may be a confounding factor preventing

966 complete anoxia (Gnaiger 2001). Chance and Williams (1955) provide an alternative definition
967 of State 5, which gives it the different meaning of ROX versus anoxia: 'State 5 may be obtained
968 by antimycin A treatment or by anaerobiosis'.
969   In **Table 3**, only States 3 and 4 are coupling control states, with the restriction that O_2
970 flux in State 3 may be limited kinetically by non-saturating ADP concentrations.

971
972

973 **3. Normalization: flows and fluxes**

974

975 *3.1. Normalization: system or sample*

976
977   The term *rate* is not sufficiently defined to be useful for reporting data (**Figure 7**). The
978 inconsistency of the meanings of rate becomes apparent when considering Galileo Galilei's
979 famous principle, that 'bodies of different weight all fall at the same rate (have a constant
980 acceleration)' (Coopersmith 2010).
981   **Flow per system, *I*:** In a generalization of electrical terms, flow as an extensive quantity
982 (*I*; per system) is distinguished from flux as a size-specific quantity (*J*; per system size) (**Figure
983 7A**). Electric current is flow, I_{el} [A ≡ C·s^{-1}] per system (extensive quantity). When dividing this
984 extensive quantity by system size (cross-sectional area of a 'wire'), a size-specific quantity is
985 obtained, which is flux (current density), J_{el} [A·m^{-2} = C·s^{-1}·m^{-2}] (**Box 2**).

986

987 **Box 2: Metabolic flows and fluxes: vectorial and scalar**
988
989   *Flows, I_{tr},* are defined for all transformations as extensive quantities. Electric charge per
990 unit time is electric flow or current, $I_{el} = dQ_{el} \cdot dt^{-1}$ [A]. When expressed per unit cross-sectional
991 area, *A* [m^2], a vector flux is obtained, which is current density (surface-density of flow)
992 perpendicular to the direction of flux, $J_{el} = I_{el} \cdot A^{-1}$ [A·m^{-2}] (Cohen et al. 2008). Fluxes with
993 *spatial* geometric direction and magnitude are *vectors*. Vector and scalar *fluxes* are related to
994 flows as $J_{tr} = I_{tr} \cdot A^{-1}$ [mol·s^{-1}·m^{-2}] and $J_{tr} = I_{tr} \cdot V^{-1}$ [mol·s^{-1}·m^{-3}], expressing flux as an area-specific
995 vector or volume-specific vectorial or scalar quantity, respectively (Gnaiger 1993b). We use
996 the metre–kilogram–second–ampere (MKSA) international system of units (*SI*) for general
997 cases ([m], [kg], [s] and [A]), with decimal *SI* prefixes for specific applications (**Table 4**).
998   We suggest to define: (*1*) *vectoral* fluxes, which are translocations as functions of
999 *gradients* with direction in geometric space in continuous systems; (*2*) *vectorial* fluxes, which
1000 describe translocations in discontinuous systems and are restricted to information on
1001 *compartmental differences* (**Figure 3**, transmembrane proton flux); and (*3*) *scalar* fluxes, which
1002 are transformations in a *homogenous* system (**Figure 3**, catabolic O_2 flux, J_{kO_2}).
1003   Vectorial transmembrane proton fluxes, J_{mH+pos} and J_{mH+neg}, are analyzed in a
1004 heterogenous compartmental system as a quantity with *directional* but not *spatial* information.
1005 Translocation of protons across the mtIM has a defined direction, either from the negative
1006 compartment (matrix space; negative, neg–compartment) to the positive compartment (inter-
1007 membrane space; positive, pos–compartment) or *vice versa* (**Figure 3**). The arrows defining
1008 the direction of the translocation between the two vesicular compartments may point upwards
1009 or downwards, right or left, without any implication that these are actual directions in space.
1010 The pos–compartment is neither above nor below the neg–compartment in a spatial sense, but
1011 can be visualized arbitrarily in a figure in the upper position (**Figure 3**). In general, the
1012 *compartmental direction* of vectorial translocation from the neg–compartment to the pos–
1013 compartment is defined by assigning the initial and final state as *ergodynamic compartments*,
1014 $H^+_{neg} \rightarrow H^+_{pos}$ or $0 = -1\ H^+_{neg} + 1\ H^+_{pos}$, related to work (erg = work) that must be performed to
1015 lift the proton from a lower to a higher electrochemical potential or from the lower to the higher
1016 ergodynamic compartment (Gnaiger 1993b).

In analogy to *vectorial* translocation, the direction of a *scalar* chemical reaction, A → B or 0 = -1 A+1 B, is defined by assigning substrates and products, A and B, as ergodynamic compartments. O_2 is defined as a substrate in respiratory O_2 consumption (electron acceptor), which together with the fuel substrates (electron donors) comprises the substrate compartment of the catabolic reaction. Volume-specific scalar O_2 flux is coupled to vectorial translocation, yielding the H^+_{pos}/O_2 ratio (**Figure 2B**).

Figure 7. Flow and flux, and normalization in structure-function analysis

(**A**) Different meanings of rate may lead to confusion, if the normalization is not sufficiently specified. Results are frequently expressed as mass-specific *flux*, J_{mX}, per mg protein, dry or wet weight (mass). Cell volume, V_{ce}, may be used for normalization (volume-specific flux, J_{Vce}), which must be clearly distinguished from flow per cell, I_{Nce}, or flux, J_V, expressed for methodological reasons per volume of the measurement system.

(**B**) O_2 flow, $I_{O_2/NX}$, is the product of performance per functional element (element function, mitochondria-specific flux), element density (mitochondrial density, D_{mtE}), and size of entity X (mass, M_X). (**b1**) Structured analysis: performance is the product of mitochondrial *function* (mt-specific flux) and *structure* (functional elements; D_{mtE} times mass of X). (**b2**) Unstructured analysis: performance is the product of *entity mass-specific flux*, $J_{O_2/MX} = I_{O_2/NX}/M_X$ [mol·s^{-1}·kg^{-1}] and *size of entity*, expressed as mass of X; $M_X = m_X \cdot N_X^{-1}$ [kg·x^{-1}]. Modified from Gnaiger (2014). For further details see **Table 4**.

Extensive quantities: An extensive quantity increases proportionally with system size. The magnitude of an extensive quantity is completely additive for non-interacting subsystems—such as mass or flow expressed per defined system. The magnitude of these quantities depends on the extent or size of the system (Cohen *et al.* 2008).

Size-specific quantities: 'The adjective *specific* before the name of an extensive quantity is often used to mean *divided by mass*' (Cohen *et al.* 2008). In this system-paradigm, mass-specific flux is flow divided by mass of the *system* (the total mass of everything within the measuring chamber or reactor). A mass-specific quantity is independent of the extent of non-
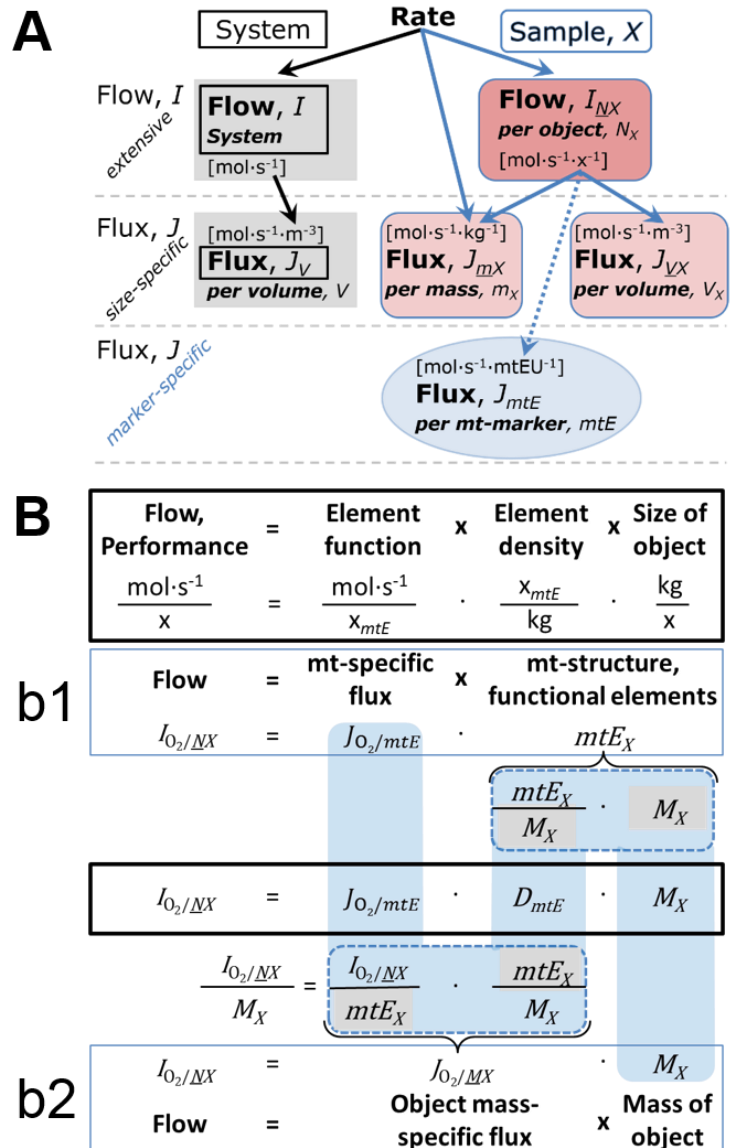
1068 interacting homogenous subsystems. Tissue-specific quantities (related to the *sample* in
1069 contrast to the *system*) are of fundamental interest in the field of comparative mitochondrial
1070 physiology, where *specific* refers to the *type of the sample* rather than *mass of the system*. The
1071 term *specific*, therefore, must be clarified; *sample*-specific, *e.g.*, muscle mass-specific
1072 normalization, is distinguished from *system*-specific quantities (mass or volume; **Figure 7**).

1074 *3.2. Normalization for system-size: flux per chamber volume*

1076 **System-specific flux, J_{V,O_2}**: The experimental system (experimental chamber) is part of
1077 the measurement apparatus, separated from the environment as an isolated, closed, open,
1078 isothermal or non-isothermal system (**Table 4**). On another level, we distinguish between (*1*)
1079 the *system* with volume V and mass m defined by the system boundaries, and (*2*) the *sample* or
1080 *objects* with volume V_X and mass m_X that are enclosed in the experimental chamber (**Figure 7**).
1081 Metabolic O_2 flow per object, $I_{O_2/\underline{N}X}$, is the total O_2 flow in the system divided by the number of
1082 objects, N_X, in the system. $I_{O_2/\underline{N}X}$ increases as the mass of the object is increased. Sample mass-
1083 specific O_2 flux, $J_{O_2/\underline{m}X}$ should be independent of the mass of the sample studied in the
1084 instrument chamber, but system volume-specific O_2 flux, J_{V,O_2} (per volume of the instrument
1085 chamber), should increase in direct proportion to the mass of the sample in the chamber.
1086 Whereas J_{V,O_2} depends on mass-concentration of the sample in the chamber, it should be
1087 independent of the chamber (system) volume at constant sample mass. There are practical
1088 limitations to increase the mass-concentration of the sample in the chamber, when one is
1089 concerned about crowding effects and instrumental time resolution.
1090 N_X and m_X indicate the number format and mass format, respectively, for expressing the
1091 quantity of a sample X. When different formats are indicated in symbols of derived quantities,
1092 the format ($\underline{N}$, $\underline{m}$) is shown as a subscript (*underlined italic*), as in $I_{O_2/\underline{N}X}$ and $J_{O_2/\underline{m}X}$. Oxygen flow
1093 and flux are expressed in the molar format, n_{O_2} [mol], but in the volume format, V_{O_2} [m^3] in
1094 ergometry. For mass-specific flux these formats can be distinguished as $J_{\underline{n}O_2/\underline{m}X}$ and $J_{\underline{V}O_2/\underline{m}X}$,
1095 respectively. Further examples are given in **Figure 7** and **Table 4**.
1096 When the reactor volume does not change during the reaction, which is typical for liquid
1097 phase reactions, the volume-specific *flux of a chemical reaction* r is the time derivative of the
1098 advancement of the reaction per unit volume, $J_{V,rB} = d_r\xi_B/dt \cdot V^{-1}$ [(mol·s^{-1})·L^{-1}]. The *rate of*
1099 *concentration change* is dc_B/dt [(mol·L^{-1})·s^{-1}], where concentration is $c_B = n_B/V$. There is a
1100 difference between (*1*) J_{V,rO_2} [mol·s^{-1}·L^{-1}] and (*2*) rate of concentration change [mol·L^{-1}·s^{-1}].
1101 These merge to a single expression only in closed systems. In open systems, external fluxes
1102 (such as O_2 supply) are distinguished from internal transformations (catabolic flux, O_2
1103 consumption). In a closed system, external flows of all substances are zero and O_2 consumption
1104 (internal flow of catabolic reactions k), I_{kO_2} [pmol·s^{-1}], causes a decline of the amount of O_2 in
1105 the system, n_{O_2} [nmol]. Normalization of these quantities for the volume of the system, V [L ≡
1106 dm^3], yields volume-specific O_2 flux, $J_{V,kO_2} = I_{kO_2}/V$ [nmol·s^{-1}·L^{-1}], and O_2 concentration, [O_2]
1107 or $c_{O_2} = n_{O_2}/V$ [μmol·L^{-1} = μM = nmol·mL^{-1}]. Instrumental background O_2 flux is due to external
1108 flux into a non-ideal closed respirometer; then total volume-specific flux has to be corrected for
1109 instrumental background O_2 flux—O_2 diffusion into or out of the instrumental chamber. J_{V,kO_2}
1110 is relevant mainly for methodological reasons and should be compared with the accuracy of
1111 instrumental resolution of background-corrected flux, *e.g.*, ±1 nmol·s^{-1}·L^{-1} (Gnaiger 2001).
1112 'Metabolic' or catabolic indicates O_2 flux, J_{kO_2}, corrected for: (*1*) instrumental background O_2
1113 flux; (*2*) chemical background O_2 flux due to autoxidation of chemical components added to
1114 the incubation medium; and (*3*) *Rox* for O_2-consuming side reactions unrelated to the catabolic
1115 pathway k.

1119 *3.3. Normalization: per sample*
1120
1121   The challenges of measuring mitochondrial respiratory flux are matched by those of
1122 normalization. Application of common and defined units is required for direct transfer of
1123 reported results into a database. The second [s] is the *SI* unit for the base quantity *time*. It is also
1124 the standard time-unit used in solution chemical kinetics. A rate may be considered as the
1125 numerator and normalization as the complementary denominator, which are tightly linked in
1126 reporting the measurements in a format commensurate with the requirements of a database.
1127 Normalization (**Table 4**) is guided by physicochemical principles, methodological
1128 considerations, and conceptual strategies (**Figure 7**).
1129
1130
1131

Table 4. Sample concentrations and normalization of flux.

Expression	Symbol	Definition	Unit	Notes
Sample				
identity of sample	X	object: cell, tissue, animal, patient		
number of sample entities X	N_X	number of objects	x	1
mass of sample X	m_X		kg	2
mass of object X	M_X	$M_X = m_X \cdot N_X^{-1}$	$kg \cdot x^{-1}$	2
Mitochondria				
Mitochondria	mt	$X = $ mt		
amount of mt-elements	mtE	quantity of mt-marker	mtEU	
Concentrations				
object number concentration	C_{NX}	$C_{NX} = N_X \cdot V^{-1}$	$x \cdot m^{-3}$	3
sample mass concentration	C_{mX}	$C_{mX} = m_X \cdot V^{-1}$	$kg \cdot m^{-3}$	
mitochondrial concentration	C_{mtE}	$C_{mtE} = mtE \cdot V^{-1}$	$mtEU \cdot m^{-3}$	4
specific mitochondrial density	D_{mtE}	$D_{mtE} = mtE \cdot m_X^{-1}$	$mtEU \cdot kg^{-1}$	5
mitochondrial content, mtE per object X	mtE_{NX}	$mtE_{NX} = mtE \cdot N_X^{-1}$	$mtEU \cdot x^{-1}$	6
O₂ flow and flux				7
flow, system	I_{O_2}	internal flow	$mol \cdot s^{-1}$	8
volume-specific flux	J_{V,O_2}	$J_{V,O_2} = I_{O_2} \cdot V^{-1}$	$mol \cdot s^{-1} \cdot m^{-3}$	9
flow per object X	$I_{O_2/NX}$	$I_{O_2/NX} = J_{V,O_2} \cdot C_{NX}^{-1}$	$mol \cdot s^{-1} \cdot x^{-1}$	10
mass-specific flux	$J_{O_2/mX}$	$J_{O_2/mX} = J_{V,O_2} \cdot C_{mX}^{-1}$	$mol \cdot s^{-1} \cdot kg^{-1}$	
mitochondria-specific flux	$J_{O_2/mtE}$	$J_{O_2/mtE} = J_{V,O_2} \cdot C_{mtE}^{-1}$	$mol \cdot s^{-1} \cdot mtEU^{-1}$	11

1132 1   The unit x for a number is not used by IUPAC. To avoid confusion, the units [$kg \cdot x^{-1}$] and [kg]
1133   distinguish the mass per object from the mass of a sample that may contain any number of objects.
1134   Similarly, the units for flow per system *versus* flow per object are [$mol \cdot s^{-1}$] (Note 8) and [$mol \cdot s^{-1} \cdot x^{-1}$]
1135   (Note 10).
1136 2   Units are given in the MKSA system (**Box 2**). The *SI* prefix k is used for the *SI* base unit of mass (kg
1137   = 1,000 g). In praxis, various *SI* prefixes are used for convenience, to make numbers easily readable,
1138   *e.g.,* 1 mg tissue, cell or mitochondrial mass instead of 0.000001 kg.
1139 3   In case of cells (sample $X = $ cells), the object number concentration is $C_{Nce} = N_{ce} \cdot V^{-1}$, and volume
1140   may be expressed in [$dm^3 \equiv L$] or [$cm^3 = mL$]. See **Table 5** for different object types.
1141 4   mt-concentration is an experimental variable, dependent on sample concentration: (*1*) $C_{mtE} = mtE \cdot V^{-1}$;
1142   (*2*) $C_{mtE} = mtE_X \cdot C_{NX}$; (*3*) $C_{mtE} = C_{mX} \cdot D_{mtE}$.
1143 5   If the amount of mitochondria, mtE, is expressed as mitochondrial mass, then D_{mtE} is the mass
1144   fraction of mitochondria in the sample. If mtE is expressed as mitochondrial volume, V_{mt}, and the

1145   mass of sample, m_X, is replaced by volume of sample, V_X, then D_{mtE} is the volume fraction of
1146   mitochondria in the sample.
1147   6 $mtE_{NX} = mtE \cdot N_X^{-1} = C_{mtE} \cdot C_{NX}^{-1}$.
1148   7 O_2 can be replaced by other chemicals B to study different reactions, *e.g.,* ATP, H_2O_2, or vesicular
1149   compartmental translocations, *e.g.,* Ca^{2+}.
1150   8 I_{O_2} and V are defined per instrument chamber as a system of constant volume (and constant
1151   temperature), which may be closed or open. I_{O_2} is abbreviated for I_{rO_2}, *i.e.*, the metabolic or internal
1152 O_2 flow of the chemical reaction r in which O_2 is consumed, hence the negative stoichiometric
1153   number, $v_{O_2} = -1$. $I_{rO_2} = d_r n_{O_2}/dt \cdot v_{O_2}^{-1}$. If r includes all chemical reactions in which O_2 participates, then
1154 $d_r n_{O_2} = dn_{O_2} - d_e n_{O_2}$, where dn_{O_2} is the change in the amount of O_2 in the instrument chamber and $d_e n_{O_2}$
1155   is the amount of O_2 added externally to the system. At steady state, by definition $dn_{O_2} = 0$, hence $d_r n_{O_2}$
1156 $= -d_e n_{O_2}$.
1157   9 J_{V,O_2} is an experimental variable, expressed per volume of the instrument chamber.
1158 10 $I_{O_2/NX}$ is a physiological variable, depending on the size of entity X.
1159 11 There are many ways to normalize for a mitochondrial marker, that are used in different experimental
1160   approaches: (*1*) $J_{O_2/mtE} = J_{V,O_2} \cdot C_{mtE}^{-1}$; (*2*) $J_{O_2/mtE} = J_{V,O_2} \cdot C_{mX}^{-1} \cdot D_{mtE}^{-1} = J_{O_2/mX} \cdot D_{mtE}^{-1}$; (*3*) $J_{O_2/mtE} =$
1161 $J_{V,O_2} \cdot C_{NX}^{-1} \cdot mtE_{NX}^{-1} = I_{O_2/NX} \cdot mtE_{NX}^{-1}$; (*4*) $J_{O_2/mtE} = I_{O_2} \cdot mtE^{-1}$. The mt-elemental unit [mtEU] varies depending
1162   on the mt-marker.

Sample concentration, C_{mX}: Normalization for sample concentration is required to report respiratory data. Considering a tissue or cells as the sample, X, the sample mass is m_X [mg], which is frequently measured as wet or dry weight, W_w or W_d [mg], respectively, or as amount of tissue or cell protein, $m_{Protein}$. In the case of permeabilized tissues, cells, and homogenates, the sample concentration, $C_{mX} = m_X/V$ [g·L^{-1} = mg·mL^{-1}], is the mass of the subsample of tissue that is transferred into the instrument chamber.

Mass-specific flux, $J_{O_2/mX}$: Mass-specific flux is obtained by expressing respiration per mass of sample, m_X [mg]. X is the type of sample—isolated mitochondria, tissue homogenate, permeabilized fibres or cells. Volume-specific flux is divided by mass concentration of X, $J_{O_2/mX} = J_{V,O_2}/C_{mX}$; or flow per cell is divided by mass per cell, $J_{O_2/mce} = I_{O_2/ce}/M_{ce}$. If mass-specific O_2 flux is constant and independent of sample size (expressed as mass), then there is no interaction between the subsystems. A 1.5 mg and a 3.0 mg muscle sample respires at identical mass-specific flux. Mass-specific O_2 flux, however, may change with the mass of a tissue sample, cells or isolated mitochondria in the measuring chamber, in which the nature of the interaction becomes an issue. Therefore, cell density must be optimized, particularly in experiments carried out in wells, considering the confluency of the cell monolayer or clumps of cells (Salabei *et al.* 2014).

Number concentration, C_{NX}: C_{NX} is the experimental *number concentration* of sample X. In the case of cells or animals, *e.g.*, nematodes, $C_{NX} = N_X/V$ [x·L^{-1}], where N_X is the number of cells or organisms in the chamber (**Table 4**).

Flow per object, $I_{O_2/NX}$: A special case of normalization is encountered in respiratory studies with permeabilized (or intact) cells. If respiration is expressed per cell, the O_2 flow per measurement system is replaced by the O_2 flow per cell, $I_{O_2/Nce}$ (**Table 4**). O_2 flow can be calculated from volume-specific O_2 flux, J_{V,O_2} [nmol·s^{-1}·L^{-1}] (per V of the measurement chamber [L]), divided by the number concentration of cells, $C_{Nce} = N_{ce}/V$ [x·L^{-1}], where N_{ce} is the number of cells in the chamber. The total cell count is the sum of viable and dead cells, $N_{ce} = N_{vce} + N_{dce}$ (**Table 5**). The cell viability index, $CVI = N_{vce}/N_{ce}$, is the ratio of viable cells (N_{vce}; before experimental permeabilization) per total cell count. After experimental permeabilization, all cells are permeabilized, $N_{pce} = N_{ce}$. The cell viability index can be used to normalize respiration for the number of cells that have been viable before experimental permeabilization, $I_{O_2/Nvce} = I_{O_2/Nce}/CVI$, considering that mitochondrial respiratory dysfunction in dead cells should be eliminated as a confounding factor.

Cellular O_2 flow can be compared between cells of identical size. To take into account changes and differences in cell size, normalization is required to obtain cell size-specific or mitochondrial marker-specific O_2 flux (Renner *et al.* 2003).

The complexity changes when the sample is a whole organism studied as an experimental model. The scaling law in respiratory physiology reveals a strong interaction of O_2 flow and individual body mass of an organism, since *basal* metabolic rate (flow) does not increase linearly with body mass, whereas *maximum* mass-specific O_2 flux, $\dot{V}_{O2max}$ or $\dot{V}_{O2peak}$, is approximately constant across a large range of individual body mass (Weibel and Hoppeler 2005), with individuals, breeds, and species deviating substantially from this relationship. For comparison of units, $\dot{V}_{O2peak}$ of human endurance athletes is 60 to 80 mL $O_2 \cdot min^{-1} \cdot kg^{-1}$ body mass, converted to $J_{O2peak/\underline{M}org}$ of 45 to 60 $nmol \cdot s^{-1} \cdot g^{-1}$ (Gnaiger 2014; **Table 6**).

Table 5. Sample types, *X*, abbreviations, and quantification.

Identity of sample mitochondrial preparation	*X*	N_X [x]	**Mass**[a] [kg]	**Volume** [m³]	**mt-Marker** [mtEU]
isolated mitochondria	imt		m_{mt}	V_{mt}	mtE
tissue homogenate	thom		m_{thom}		mtE_{thom}
permeabilized tissue	pti		m_{pti}		mtE_{pti}
permeabilized fibre	pfi		m_{pfi}		mtE_{pfi}
permeabilized cell	pce	N_{pce}	M_{pce}	V_{pce}	mtE_{pce}
cells[b]	ce	N_{ce}	M_{ce}	V_{ce}	mtE_{ce}
intact cell, viable cell	vce	N_{vce}	M_{vce}	V_{vce}	
dead cell	dce	N_{dce}	M_{dce}	V_{dce}	
organism	org	N_{org}	M_{org}	V_{org}	

[a] Instead of mass, the wet weight or dry weight is frequently stated, W_w or W_d. m_X is mass of the sample [kg], M_X is mass of the object [kg·x⁻¹] (**Table 4**).

[b] Total cell count, $N_{ce} = N_{vce} + N_{dce}$

3.4. Normalization for mitochondrial content

Tissues can contain multiple cell populations that may have distinct mitochondrial subtypes. Mitochondria undergo dynamic fission and fusion cycles, and can exist in multiple stages and sizes that may be altered by a range of factors. The isolation of mitochondria (often achieved through differential centrifugation) can therefore yield a subsample of the mitochondrial types present in a tissue, depending on the isolation protocols utilized (*e.g.,* centrifugation speed). This possible bias should be taken into account when planning experiments using isolated mitochondria. Different sizes of mitochondria are enriched at specific centrifugation speeds, which can be used strategically for isolation of mitochondrial subpopulations.

Part of the mitochondrial content of a tissue is lost during preparation of isolated mitochondria. The fraction of isolated mitochondria obtained from a tissue sample is expressed as mitochondrial recovery. At a high mitochondrial recovery the fraction of isolated mitochondria is more representative of the total mitochondrial population than in preparations characterized by low recovery. Determination of the mitochondrial recovery and yield is based on measurement of the concentration of a mitochondrial marker in the stock of isolated mitochondria, $C_{mtE,stock}$, and crude tissue homogenate, $C_{mtE,thom}$, which simultaneously provides information on the specific mitochondrial density in the sample, D_{mtE} (**Table 4**).

Normalization is a problematic subject; it is essential to consider the question of the study. If the study aims at comparing tissue performance—such as the effects of a treatment on a specific tissue, then normalization for tissue mass or protein content is appropriate. However, if the aim is to find differences on mitochondrial function independent of mitochondrial density (**Table 4**), then normalization to a mitochondrial marker is imperative (**Figure 7**). One cannot

assume that quantitative changes in various markers—such as mitochondrial proteins—necessarily occur in parallel with one another. It should be established that the marker chosen is not selectively altered by the performed treatment. In conclusion, the normalization must reflect the question under investigation to reach a satisfying answer. On the other hand, the goal of comparing results across projects and institutions requires standardization on normalization for entry into a databank.

Mitochondrial concentration, C_{mtE}, and mitochondrial markers: Mitochondrial organelles comprise a dynamic cellular reticulum in various states of fusion and fission. Hence, the definition of an "amount" of mitochondria is often misconceived: mitochondria cannot be counted reliably as a number of occurring elements. Therefore, quantification of the "amount" of mitochondria depends on the measurement of chosen mitochondrial markers. 'Mitochondria are the structural and functional elemental units of cell respiration' (Gnaiger 2014). The quantity of a mitochondrial marker can reflect the amount of *mitochondrial elements*, *mtE*, expressed in various mitochondrial elemental units [mtEU] specific for each measured mt-marker (**Table 4**). However, since mitochondrial quality may change in response to stimuli—particularly in mitochondrial dysfunction (Campos *et al.* 2017) and after exercise training (Pesta *et al.* 2011) and during aging (Daum *et al.* 2013)—some markers can vary while others are unchanged: (*1*) Mitochondrial volume and membrane area are structural markers, whereas mitochondrial protein mass is frequently used as a marker for isolated mitochondria. (*2*) Molecular and enzymatic mitochondrial markers (amounts or activities) can be selected as matrix markers, *e.g.*, citrate synthase activity, mtDNA; mtIM-markers, *e.g.*, cytochrome *c* oxidase activity, aa_3 content, cardiolipin, or mtOM-markers, *e.g.*, the voltage-dependent anion channel (VDAC), TOM20. (*3*) Extending the measurement of mitochondrial marker enzyme activity to mitochondrial pathway capacity, ET- or OXPHOS-capacity can be considered as an integrative functional mitochondrial marker.

Depending on the type of mitochondrial marker, the mitochondrial elements, *mtE*, are expressed in marker-specific units. Mitochondrial concentration in the measurement chamber and the tissue of origin are quantified as (*1*) a quantity for normalization in functional analyses, C_{mtE}, and (*2*) a physiological output that is the result of mitochondrial biogenesis and degradation, D_{mtE}, respectively (**Table 4**). It is recommended, therefore, to distinguish *experimental mitochondrial concentration*, $C_{mtE} = mtE/V$ and *physiological mitochondrial density*, $D_{mtE} = mtE/m_X$. Then mitochondrial density is the amount of mitochondrial elements per mass of tissue, which is a biological variable (**Figure 7**). The experimental variable is mitochondrial density multiplied by sample mass concentration in the measuring chamber, $C_{mtE} = D_{mtE} \cdot C_{mX}$, or mitochondrial content multiplied by sample number concentration, $C_{mtE} = mtE_X \cdot C_{NX}$ (**Table 4**).

Mitochondria-specific flux, $J_{O_2/mtE}$: Volume-specific metabolic O_2 flux depends on: (*1*) the sample concentration in the volume of the instrument chamber, C_{mX}, or C_{NX}; (*2*) the mitochondrial density in the sample, $D_{mtE} = mtE/m_X$ or $mtE_X = mtE/N_X$; and (*3*) the specific mitochondrial activity or performance per elemental mitochondrial unit, $J_{O_2/mtE} = J_{V,O_2}/C_{mtE}$ [mol·s^{-1}·mtEU^{-1}] (**Table 4**). Obviously, the numerical results for $J_{O_2/mtE}$ vary with the type of mitochondrial marker chosen for measurement of *mtE* and $C_{mtE} = mtE/V$ [mtEU·m^{-3}].

3.5. Evaluation of mitochondrial markers

Different methods are implicated in the quantification of mitochondrial markers and have different strengths. Some problems are common for all mitochondrial markers, *mtE*: (*1*) Accuracy of measurement is crucial, since even a highly accurate and reproducible measurement of O_2 flux results in an inaccurate and noisy expression if normalized by a biased and noisy measurement of a mitochondrial marker. This problem is acute in mitochondrial respiration because the denominators used (the mitochondrial markers) are often small moieties

of which accurate and precise determination is difficult. This problem can be avoided when O_2 fluxes measured in substrate-uncoupler-inhibitor titration protocols are normalized for flux in a defined respiratory reference state, which is used as an *internal* marker and yields flux control ratios, *FCR*s. *FCR*s are independent of *externally* measured markers and, therefore, are statistically robust, considering the limitations of ratios in general (Jasienski and Bazzaz 1999). *FCR*s indicate qualitative changes of mitochondrial respiratory control, with highest quantitative resolution, separating the effect of mitochondrial density or concentration on $J_{O_2/mX}$ and $I_{O_2/\underline{NX}}$ from that of function per elemental mitochondrial marker, $J_{O_2/mtE}$ (Pesta *et al.* 2011; Gnaiger 2014). (*2*) If mitochondrial quality does not change and only the amount of mitochondria varies as a determinant of mass-specific flux, any marker is equally qualified in principle; then in practice selection of the optimum marker depends only on the accuracy and precision of measurement of the mitochondrial marker. (*3*) If mitochondrial flux control ratios change, then there may not be any best mitochondrial marker. In general, measurement of multiple mitochondrial markers enables a comparison and evaluation of normalization for a variety of mitochondrial markers. Particularly during postnatal development, the activity of marker enzymes—such as cytochrome *c* oxidase and citrate synthase—follows different time courses (Drahota *et al.* 2004). Evaluation of mitochondrial markers in healthy controls is insufficient for providing guidelines for application in the diagnosis of pathological states and specific treatments.

In line with the concept of the respiratory control ratio (Chance and Williams 1955a), the most readily used normalization is that of flux control ratios and flux control factors (Gnaiger 2014). Selection of the state of maximum flux in a protocol as the reference state has the advantages of: (*1*) internal normalization; (*2*) statistically validated linearization of the response in the range of 0 to 1; and (*3*) consideration of maximum flux for integrating a large number of elemental steps in the OXPHOS- or ET-pathways. This reduces the risk of selecting a functional marker that is specifically altered by the treatment or pathology, yet increases the chance that the highly integrative pathway is disproportionately affected, *e.g.,* the OXPHOS- rather than ET-pathway in case of an enzymatic defect in the phosphorylation-pathway. In this case, additional information can be obtained by reporting flux control ratios based on a reference state which indicates stable tissue-mass specific flux.

Stereological determination of mitochondrial content via two-dimensional transmission electron microscopy can have limitations due to the dynamics of mitochondrial size (Meinild Lundby *et al.* 2017). Accurate determination of three-dimensional volume by two-dimensional microscopy can be both time consuming and statistically challenging (Larsen *et al.* 2012).

The validity of using mitochondrial marker enzymes (citrate synthase activity, Complex I–IV amount or activity) for normalization of flux is limited in part by the same factors that apply to flux control ratios. Strong correlations between various mitochondrial markers and citrate synthase activity (Reichmann *et al.* 1985; Boushel *et al.* 2007; Mogensen *et al.* 2007) are expected in a specific tissue of healthy persons and in disease states not specifically targeting citrate synthase. Citrate synthase activity is acutely modifiable by exercise (Tonkonogi *et al.* 1997; Leek *et al.* 2001). Evaluation of mitochondrial markers related to a selected age and sex cohort cannot be extrapolated to provide recommendations for normalization in respirometric diagnosis of disease, in different states of development and ageing, different cell types, tissues, and species. mtDNA normalized to nDNA via qPCR is correlated to functional mitochondrial markers including OXPHOS- and ET-capacity in some cases (Puntschart *et al.* 1995; Wang *et al.* 1999; Menshikova *et al.* 2006; Boushel *et al.* 2007; Ehinger *et al.* 2015), but lack of such correlations have been reported (Menshikova *et al.* 2005; Schultz and Wiesner 2000; Pesta *et al.* 2011). Several studies indicate a strong correlation between cardiolipin content and increase in mitochondrial function with exercise (Menshikova *et al.* 2005; Menshikova *et al.* 2007; Larsen *et al.* 2012; Faber *et al.* 2014), but it has not been evaluated as a general mitochondrial biomarker in disease. With no single best mitochondrial

marker, a good strategy is to quantify several different biomarkers to minimize the decorrelating effects caused by diseases, treatments, or other factors. Determination of multiple markers, particularly a matrix marker and a marker from the mtIM, allows tracking changes in mitochondrial quality defined by their ratio.

3.6. Conversion: units

Many different units have been used to report the O_2 consumption rate, OCR (**Table 6**). *SI* base units provide the common reference to introduce the theoretical principles (**Figure 7**), and are used with appropriately chosen *SI* prefixes to express numerical data in the most practical format, with an effort towards unification within specific areas of application (**Table 7**). Reporting data in *SI* units—including the mole [mol], coulomb [C], joule [J], and second [s]—should be encouraged, particularly by journals which propose the use of *SI* units.

Table 6. Conversion of various formats and units used in respirometry and ergometry. e^- is the number of electrons or reducing equivalents. z_B is the charge number of entity B.

Format	1 Unit	·	Multiplication factor	SI-unit	Note
n	ng.atom O·s^{-1}	(2 e$^-$)	0.5	nmol O$_2$·s^{-1}	
n	ng.atom O·min^{-1}	(2 e$^-$)	8.33	pmol O$_2$·s^{-1}	
n	natom O·min^{-1}	(2 e$^-$)	8.33	pmol O$_2$·s^{-1}	
n	nmol O$_2$·min^{-1}	(4 e$^-$)	16.67	pmol O$_2$·s^{-1}	
n	nmol O$_2$·h^{-1}	(4 e$^-$)	0.2778	pmol O$_2$·s^{-1}	
V to n	mL O$_2$·min^{-1} at STPD^a		0.744	µmol O$_2$·s^{-1}	1
e to n	W = J/s at -470 kJ/mol O$_2$		-2.128	µmol O$_2$·s^{-1}	
e to n	mA = mC·s^{-1}	(z_{H^+} = 1)	10.36	nmol H$^+$·s^{-1}	2
e to n	mA = mC·s^{-1}	(z_{O_2} = 4)	2.59	nmol O$_2$·s^{-1}	2
n to e	nmol H$^+$·s^{-1}	(z_{H^+} = 1)	0.09649	mA	3
n to e	nmol O$_2$·s^{-1}	(z_{O_2} = 4)	0.38594	mA	3

1 At standard temperature and pressure dry (STPD: 0 °C = 273.15 K and 1 atm = 101.325 kPa = 760 mmHg), the molar volume of an ideal gas, V_m, and V_{m,O_2} is 22.414 and 22.392 L·mol^{-1}, respectively. Rounded to three decimal places, both values yield the conversion factor of 0.744. For comparison at normal temperature and pressure dry (NTPD: 20 °C), V_{m,O_2} is 24.038 L·mol^{-1}. Note that the *SI* standard pressure is 100 kPa.
2 The multiplication factor is $10^6/(z_B·F)$.
3 The multiplication factor is $z_B·F/10^6$.

Although volume is expressed as m^3 using the *SI* base unit, the litre [dm^3] is a conventional unit of volume for concentration and is used for most solution chemical kinetics. If one multiplies $I_{O_2/Nce}$ by C_{Nce}, then the result will not only be the amount of O_2 [mol] consumed per time [s^{-1}] in one litre [L^{-1}], but also the change in O_2 concentration per second (for any volume of an ideally closed system). This is ideal for kinetic modeling as it blends with chemical rate equations where concentrations are typically expressed in mol·L^{-1} (Wagner *et al.* 2011). In studies of multinuclear cells—such as differentiated skeletal muscle cells—it is easy to determine the number of nuclei but not the total number of cells. A generalized concept, therefore, is obtained by substituting cells by nuclei as the sample entity. This does not hold, however, for enucleated platelets.

For studies of cells, we recommend that respiration be expressed, as far as possible, as: (*1*) O₂ flux normalized for a mitochondrial marker, for separation of the effects of mitochondrial quality and content on cell respiration (this includes *FCR*s as a normalization for a functional mitochondrial marker); (*2*) O₂ flux in units of cell volume or mass, for comparison of respiration of cells with different cell size (Renner *et al.* 2003) and with studies on tissue preparations, and (*3*) O₂ flow in units of attomole (10^{-18} mol) of O₂ consumed in a second by each cell [amol·s^{-1}·cell^{-1}], numerically equivalent to [pmol·s^{-1}·10^{-6} cells]. This convention allows information to be easily used when designing experiments in which O₂ flow must be considered. For example, to estimate the volume-specific O₂ flux in an instrument chamber that would be expected at a particular cell number concentration, one simply needs to multiply the flow per cell by the number of cells per volume of interest. This provides the amount of O₂ [mol] consumed per time [s^{-1}] per unit volume [L^{-1}]. At an O₂ flow of 100 amol·s^{-1}·cell^{-1} and a cell density of 10^9 cells·L^{-1} (10^6 cells·mL^{-1}), the volume-specific O₂ flux is 100 nmol·s^{-1}·L^{-1} (100 pmol·s^{-1}·mL^{-1}).

Table 7. Conversion of units with preservation of numerical values.

Name	Frequently used unit	Equivalent unit	Note
volume-specific flux, J_{V,O_2}	pmol·s^{-1}·mL^{-1}	nmol·s^{-1}·L^{-1}	1
	mmol·s^{-1}·L^{-1}	mol·s^{-1}·m^{-3}	
cell-specific flow, $I_{O_2/cell}$	pmol·s^{-1}·10^{-6} cells	amol·s^{-1}·cell^{-1}	2
	pmol·s^{-1}·10^{-9} cells	zmol·s^{-1}·cell^{-1}	3
cell number concentration, C_{Nce}	10^6 cells·mL^{-1}	10^9 cells·L^{-1}	
mitochondrial protein concentration, C_{mtE}	0.1 mg·mL^{-1}	0.1 g·L^{-1}	
mass-specific flux, $J_{O_2/m}$	pmol·s^{-1}·mg^{-1}	nmol·s^{-1}·g^{-1}	4
catabolic power, P_k	μW·10^{-6} cells	pW·cell^{-1}	1
Volume	1,000 L	m^3 (1,000 kg)	
	L	dm^3 (kg)	
	mL	cm^3 (g)	
	μL	mm^3 (mg)	
	fL	μm^3 (pg)	5
amount of substance concentration	M = mol·L^{-1}	mol·dm^{-3}	

1 pmol: picomole = 10^{-12} mol   4 nmol: nanomole = 10^{-9} mol
2 amol: attomole = 10^{-18} mol   5 fL: femtolitre = 10^{-15} L
3 zmol: zeptomole = 10^{-21} mol

ET-capacity in human cell types including HEK 293, primary HUVEC and fibroblasts ranges from 50 to 180 amol·s^{-1}·cell^{-1}, measured in intact cells in the noncoupled state (see Gnaiger 2014). At 100 amol·s^{-1}·cell^{-1} corrected for *Rox*, the current across the mt-membranes, I_{H+e}, approximates 193 pA·cell^{-1} or 0.2 nA per cell. See Rich (2003) for an extension of quantitative bioenergetics from the molecular to the human scale, with a transmembrane proton flux equivalent to 520 A in an adult at a catabolic power of -110 W. Modelling approaches illustrate the link between protonmotive force and currents (Willis *et al.* 2016).

We consider isolated mitochondria as powerhouses and proton pumps as molecular machines to relate experimental results to energy metabolism of the intact cell. The cellular P»/O₂ based on oxidation of glycogen is increased by the glycolytic (fermentative) substrate-level phosphorylation of 3 P»/Glyc or 0.5 mol P» for each mol O₂ consumed in the complete oxidation of a mol glycosyl unit (Glyc). Adding 0.5 to the mitochondrial P»/O₂ ratio of 5.4 yields a bioenergetic cell physiological P»/O₂ ratio close to 6. Two NADH equivalents are

1409 formed during glycolysis and transported from the cytosol into the mitochondrial matrix, either
1410 by the malate-aspartate shuttle or by the glycerophosphate shuttle (**Figure 2A**) resulting in
1411 different theoretical yields of ATP generated by mitochondria, the energetic cost of which
1412 potentially must be taken into account. Considering also substrate-level phosphorylation in the
1413 TCA cycle, this high P»/O$_2$ ratio not only reflects proton translocation and OXPHOS studied
1414 in isolation, but integrates mitochondrial physiology with energy transformation in the living
1415 cell (Gnaiger 1993a).

4. Conclusions

1419 Catabolic cell respiration is the process of exergonic and exothermic energy
1420 transformation in which scalar redox reactions are coupled to vectorial ion translocation across
1421 a semipermeable membrane, which separates the small volume of a bacterial cell or
1422 mitochondrion from the larger volume of its surroundings. The electrochemical exergy can be
1423 partially conserved in the phosphorylation of ADP to ATP or in ion pumping, or dissipated in
1424 an electrochemical short-circuit. Respiration is thus clearly distinguished from fermentation as
1425 the counterpart of cellular core energy metabolism. An O$_2$ flux balance scheme illustrates the
1426 relationships and general definitions (**Figures 1 and 2**).
1427 Experimentally, respiration is separated in mitochondrial preparations from the
1428 interactions with the fermentative pathways of the intact cell. OXPHOS analysis (**Figure 3**) is
1429 based on the study of mitochondrial preparations complementary to bioenergetic investigations
1430 of intact cells and organisms—from model organisms to the human species including healthy
1431 and diseased persons (patients). Different mechanisms of respiratory uncoupling have to be
1432 distinguished (**Figure 4**). Metabolic fluxes measured in defined coupling and pathway control
1433 states (**Figures 5 and 6**) provide insights into the meaning of cellular and organismic
1434 respiration.
1435 The optimal choice for expressing mitochondrial and cell respiration as O$_2$ flow per
1436 biological sample, and normalization for specific tissue-markers (volume, mass, protein) and
1437 mitochondrial markers (volume, protein, content, mtDNA, activity of marker enzymes,
1438 respiratory reference state) is guided by the scientific question under study. Interpretation of
1439 the data depends critically on appropriate normalization (**Figure 7**).
1440 MitoEAGLE can serve as a gateway to better diagnose mitochondrial respiratory
1441 adaptations and defects linked to genetic variation, age-related health risks, sex-specific
1442 mitochondrial performance, lifestyle with its effects on degenerative diseases, and thermal and
1443 chemical environment. The present recommendations on coupling control states and rates,
1444 linked to the concept of the protonmotive force, are focused on studies with mitochondrial
1445 preparations (**Box 3**). These will be extended in a series of reports on pathway control of
1446 mitochondrial respiration, respiratory states in intact cells, and harmonization of experimental
1447 procedures.

1450 **Box 3: Recommendations for studies with mitochondrial preparations**

1452 ● Normalization of respiratory rates should be provided as far as possible:
1453   1. *Biophysical normalization*: on a per cell basis as O$_2$ flow; this may not be possible
1454   when dealing with coenocytic organisms or tissues without cross-walls
1455   separating individual cells (*e.g.*, filamentous fungi, muscle fibers)
1456   2. *Cellular normalization*: per g protein; per cell- or tissue-mass as mass-specific
1457   O$_2$ flux; per cell volume as cell volume-specific flux
1458   3. *Mitochondrial normalization*: per mitochondrial marker as mt-specific flux.

1459 With information on cell size and the use of multiple normalizations, maximum potential
1460 information is available (Renner *et al.* 2003; Wagner *et al.* 2011; Gnaiger 2014). Reporting
1461 flow in a respiratory chamber [nmol·s^{-1}] is discouraged, since it restricts the analysis to intra-
1462 experimental comparison of relative (qualitative) differences.

1463 ● Catabolic mitochondrial respiration is distinguished from residual O_2 consumption. Fluxes
1464 in mitochondrial coupling states should be, as far as possible, corrected for residual O_2
1465 consumption.

1466 ● Different mechanisms of uncoupling should be distinguished by defined terms. The tightness
1467 of coupling relates to these uncoupling mechanisms, whereas the coupling stoichiometry
1468 varies as a function the substrate type involved in ET-pathways with either three or two
1469 redox proton pumps operating in series. Separation of tightness of coupling from the
1470 pathway-dependent coupling stoichiometry is possible only when the substrate type
1471 undergoing oxidation remains the same for respiration in LEAK-, OXPHOS-, and ET-states.
1472 In studies of the tightness of coupling, therefore, simple substrate-inhibitor combinations
1473 should be applied to exlcude a shift in substrate competition which may occur when
1474 providing physiological substrate cocktails.

1475 ● In studies of isolated mitochondria, the mitochondrial recovery and yield should be reported.
1476 Experimental criteria for evaluation of purity versus integrity should be considered.
1477 Mitochondrial markers—such as citrate synthase activity as an enzymatic matrix marker—
1478 provide a link to the tissue of origin on the basis of calculating the mitochondrial recovery,
1479 *i.e.*, the fraction of mitochondrial marker obtained from a unit mass of tissue. Total
1480 mitochondrial protein is frequently applied as a mitochondrial marker, which is restricted to
1481 isolated mitochondria.

1482 ● In studies of permeabilized cells, the viability of the cell culture or cell suspension of origin
1483 should be reported. Normalization should be evaluated for total cell count or viable cell
1484 count.

1485 ● Terms and symbols are summarized in **Table 8**. Their use will facilitate transdisciplinary
1486 communication and support further developments towards a consistent theory of
1487 bioenergetics and mitochondrial physiology. Technical terms related to and defined with
1488 normal words can be used as index terms in databases, support the creation of ontologies
1489 towards semantic information processing (MitoPedia), and help in communicating analytical
1490 findings as impactful data-driven stories. '*Making data available without making it*
1491 *understandable may be worse than not making it available at all*' (National Academies of
1492 Sciences, Engineering, and Medicine 2018). Success will depend on taking next steps: (*1*)
1493 exhaustive text-mining considering Omics data and functional data; (*2*) network analysis of
1494 Omics data with bioinformatics tools; (*3*) cross-validation with distinct bioinformatics
1495 approaches; (*4*) correlation with functional data; (*5*) guidelines for biological validation of
1496 network data. This is a call to carefully contribute to FAIR principles (Findable, Accessible,
1497 Interoperable, Reusable) for the sharing of scientific data.

Table 8. Terms, symbols, and units.

Term	Symbol	Unit	Links and comments
alternative quinol oxidase	AOX		Figure 2B
amount of substance B	n_B	[mol]	
ATP yield per O_2	$Y_{P»/O_2}$		P»/O2 ratio measured in any respiratory state
catabolic reaction	k		Figure 1 and 3

1513	catabolic respiration	J_{kO_2}	varies	Figure 1 and 3
1514	cell number	N_{ce}	[x]	Table 5; $N_{ce} = N_{vce} + N_{dce}$
1515	cell respiration	J_{rO_2}	varies	Figure 1
1516	cell viability index	CVI		$CVI = N_{vce}/N_{ce} = 1 - N_{dce}/N_{ce}$
1517	Complexes I to IV	CI to CIV		respiratory ET Complexes; Figure 2B
1518	concentration of substance B	$c_B = n_B \cdot V^{-1}$; [B]	[mol·m^{-3}]	Box 2
1519	dead cell number	N_{dce}	[x]	Table 5; non-viable cells, loss of plasma
1520				membrane barrier function
1521	electric format	$\underline{e}$	[C]	Table 6
1522	electron transfer system	ETS		Figure 2B, Figure 5; state
1523	flow, for substance B	I_B	[mol·s^{-1}]	system-related extensive quantity;
1524				Figure 7
1525	flux, for substance B	J_B	varies	size-specific quantitiy; Figure 7
1526	inorganic phosphate	P_i		Figure 3
1527	intact cell number, viable cell number	N_{vce}	[x]	Table 5; viable cells, intact of plasma
1528				membrane barrier function
1529	LEAK	LEAK		Table 1, Figure 5; state
1530	mass format	$\underline{m}$	[kg]	Table 4, Figure 7
1531	mass of sample X	m_X	[kg]	Table 4
1532	mass of entity X	M_X	[kg]	mass of object X; Table 4
1533	MITOCARTA			https://www.broadinstitute.org/scientific-
1534				community/science/programs/metabolic
1535				-disease-
1536				program/publications/mitocarta/mitocart
1537				a-in-0
1538	MitoPedia			http://www.bioblast.at/index.php/MitoPedia
1539	mitochondria or mitochondrial	mt		Box 1
1540	mitochondrial DNA	mtDNA		Box 1
1541	mitochondrial concentration	$C_{mtE} = mtE \cdot V^{-1}$	[mtEU·m^{-3}]	Table 4
1542	mitochondrial content	$mtE_X = mtE \cdot N_X^{-1}$	[mtEU·x^{-1}]	Table 4
1543	mitochondrial element	mtE	[mtEU]	Table 4, quantity of mt-marker
1544	mitochondrial elemental unit	mtEU	varies	Table 4, specific units for mt-marker
1545	mitochondrial inner membrane	mtIM		Figure 2; MIM is widely used; the first
1546				M is replaced by mt; Box 1
1547	mitochondrial outer membrane	mtOM		Figure 2; MOM is widely used; the first
1548				M is replaced by mt; Box 1
1549	mitochondrial recovery	Y_{mtE}		fraction of mtE recovered in sample
1550				from the tissue of origin
1551	mitochondrial yield	$Y_{mtE/\underline{m}}$		mt-yield per tissues mass; $Y_{mtE/\underline{m}} = Y_{mtE} \cdot$
1552				D_{mtE}
1553	molar format	$\underline{n}$	[mol]	Table 6
1554	negative	neg		Figure 3
1555	number concentration of X	C_{NX}	[x·m^{-3}]	Table 4
1556	number format	$\underline{N}$	[x]	Table 4, Figure 7
1557	number of entities X	N_X	[x]	Table 4, Figure 7
1558	number of entity B	N_B	[x]	Table 4
1559	oxidative phosphorylation	OXPHOS		Table 1, Figure 5; state
1560	oxygen concentration	$c_{O_2} = n_{O_2} \cdot V^{-1}$; [O$_2$]	[mol·m^{-3}]	Section 3.2
1561	oxygen flux, in reaction r	J_{rO_2}	varies	Figure 1
1562	permeabilized cell number	N_{pce}	[x]	Table 5; experimental permeabilization
1563				of plasma membrane; $N_{pce} = N_{ce}$
1564	phosphorylation of ADP to ATP	P»		Section 2.2
1565	positive	pos		Figure 3
1566	proton in the negative compartment	H$^+_{neg}$		Figure 3
1567	proton in the positive compartment	H$^+_{pos}$		Figure 3
1568	rate of electron transfer in ET state	E		ET-capacity; Table 1
1569	rate of LEAK respiration	L		Table 1
1570	rate of oxidative phosphorylation	P		OXPHOS capacity; Table 1
1571	rate of residual oxygen consumption	Rox		Table 1, Figure 1
1572	residual oxygen consumption	ROX		Table 1; state

respiratory supercomplex	SC I$_n$III$_n$IV$_n$		Box 1; supramolecular assemblies composed of variable copy numbers (n) of CI, CIII and CIV
specific mitochondrial density	$D_{mtE} = mtE \cdot m_X^{-1}$	[mtEU·kg^{-1}]	Table 4
volume	V	[m^{-3}]	Table 7
volume format	$\underline{V}$	[m^{-3}]	Table 6
weight, dry weight	W_d	[kg]	used as mass of sample X; Figure 7
weight, wet weight	W_w	[kg]	used as mass of sample X; Figure 7

Acknowledgements

References

Altmann R (1894) Die Elementarorganismen und ihre Beziehungen zu den Zellen. Zweite vermehrte Auflage. Verlag Von Veit & Comp, Leipzig:160 pp.

Baggeto LG, Testa-Perussini R (1990) Role of acetoin on the regulation of intermediate metabolism of Ehrlich ascites tumor mitochondria: its contribution to membrane cholesterol enrichment modifying passive proton permeability. Arch Biochem Biophys 283:341-8.

Beard DA (2005) A biophysical model of the mitochondrial respiratory system and oxidative phosphorylation. PLoS Comput Biol 1(4):e36.

Benda C (1898) Weitere Mitteilungen über die Mitochondria. Verh Dtsch Physiol Ges:376-83.

Birkedal R, Laasmaa M, Vendelin M (2014) The location of energetic compartments affects energetic communication in cardiomyocytes. Front Physiol 5:376.

Blier PU, Dufresne F, Burton RS (2001) Natural selection and the evolution of mtDNA-encoded peptides: evidence for intergenomic co-adaptation. Trends Genet 17:400-6.

Blier PU, Guderley HE (1993) Mitochondrial activity in rainbow trout red muscle: the effect of temperature on the ADP-dependence of ATP synthesis. J Exp Biol 176:145-58.

Breton S, Beaupré HD, Stewart DT, Hoeh WR, Blier PU (2007) The unusual system of doubly uniparental inheritance of mtDNA: isn't one enough? Trends Genet 23:465-74.

Brown GC (1992) Control of respiration and ATP synthesis in mammalian mitochondria and cells. Biochem J 284:1-13.

Calvo SE, Klauser CR, Mootha VK (2016) MitoCarta2.0: an updated inventory of mammalian mitochondrial proteins. Nucleic Acids Research 44:D1251-7.

Calvo SE, Julien O, Clauser KR, Shen H, Kamer KJ, Wells JA, Mootha VK (2017) Comparative analysis of mitochondrial N-termini from mouse, human, and yeast. Mol Cell Proteomics 16:512-23.

Campos JC, Queliconi BB, Bozi LHM, Bechara LRG, Dourado PMM, Andres AM, Jannig PR, Gomes KMS, Zambelli VO, Rocha-Resende C, Guatimosim S, Brum PC, Mochly-Rosen D, Gottlieb RA, Kowaltowski AJ, Ferreira JCB (2017) Exercise reestablishes autophagic flux and mitochondrial quality control in heart failure. Autophagy 13:1304-317.

Canton M, Luvisetto S, Schmehl I, Azzone GF (1995) The nature of mitochondrial respiration and discrimination between membrane and pump properties. Biochem J 310:477-81.

Carrico C, Meyer JG, He W, Gibson BW, Verdin E (2018) The mitochondrial acylome emerges: proteomics, regulation by Sirtuins, and metabolic and disease implications. Cell Metab 27:497-512.

Chan DC (2006) Mitochondria: dynamic organelles in disease, aging, and development. Cell 125:1241-52.

Chance B, Williams GR (1955a) Respiratory enzymes in oxidative phosphorylation. I. Kinetics of oxygen utilization. J Biol Chem 217:383-93.

Chance B, Williams GR (1955b) Respiratory enzymes in oxidative phosphorylation: III. The steady state. J Biol Chem 217:409-27.

Chance B, Williams GR (1955c) Respiratory enzymes in oxidative phosphorylation. IV. The respiratory chain. J Biol Chem 217:429-38.

Chance B, Williams GR (1956) The respiratory chain and oxidative phosphorylation. Adv Enzymol Relat Subj Biochem 17:65-134.

Chowdhury SK, Djordjevic J, Albensi B, Fernyhough P (2015) Simultaneous evaluation of substrate-dependent oxygen consumption rates and mitochondrial membrane potential by TMRM and safranin in cortical mitochondria. Biosci Rep 36:e00286.

Cobb LJ, Lee C, Xiao J, Yen K, Wong RG, Nakamura HK, Mehta HH, Gao Q, Ashur C, Huffman DM, Wan J, Muzumdar R, Barzilai N, Cohen P (2016) Naturally occurring mitochondrial-derived peptides are age-dependent regulators of apoptosis, insulin sensitivity, and inflammatory markers. Aging (Albany NY) 8:796-809.

Cohen ER, Cvitas T, Frey JG, Holmström B, Kuchitsu K, Marquardt R, Mills I, Pavese F, Quack M, Stohner J, Strauss HL, Takami M, Thor HL (2008) Quantities, units and smbols in physical chemistry, IUPAC Green Book, 3rd Edition, 2nd Printing, IUPAC & RSC Publishing, Cambridge.

Cooper H, Hedges LV, Valentine JC, eds (2009) The handbook of research synthesis and meta-analysis. Russell Sage Foundation.

Coopersmith J (2010) Energy, the subtle concept. The discovery of Feynman's blocks from Leibnitz to Einstein. Oxford University Press:400 pp.

Cummins J (1998) Mitochondrial DNA in mammalian reproduction. Rev Reprod 3:172-82.

Dai Q, Shah AA, Garde RV, Yonish BA, Zhang L, Medvitz NA, Miller SE, Hansen EL, Dunn CN, Price TM (2013) A truncated progesterone receptor (PR-M) localizes to the mitochondrion and controls cellular respiration. Mol Endocrinol 27:741-53.

Daum B, Walter A, Horst A, Osiewacz HD, Kühlbrandt W (2013) Age-dependent dissociation of ATP synthase dimers and loss of inner-membrane cristae in mitochondria. Proc Natl Acad Sci U S A 110:15301-6.

Divakaruni AS, Brand MD (2011) The regulation and physiology of mitochondrial proton leak. Physiology (Bethesda) 26:192-205.

Doerrier C, Garcia-Souza LF, Krumschnabel G, Wohlfarter Y, Mészáros AT, Gnaiger E (2018) High-Resolution FluoRespirometry and OXPHOS protocols for human cells, permeabilized fibres from small biopsies of muscle, and isolated mitochondria. Methods Mol Biol 1782 (Palmeira CM, Moreno AJ, eds): Mitochondrial Bioenergetics, 978-1-4939-7830-4.

Doskey CM, van 't Erve TJ, Wagner BA, Buettner GR (2015) Moles of a substance per cell is a highly informative dosing metric in cell culture. PLOS ONE 10:e0132572.

Drahota Z, Milerová M, Stieglerová A, Houstek J, Ostádal B (2004) Developmental changes of cytochrome c oxidase and citrate synthase in rat heart homogenate. Physiol Res 53:119-22.

Duarte FV, Palmeira CM, Rolo AP (2014) The role of microRNAs in mitochondria: small players acting wide. Genes (Basel) 5:865-86.

Ehinger JK, Morota S, Hansson MJ, Paul G, Elmér E (2015) Mitochondrial dysfunction in blood cells from amyotrophic lateral sclerosis patients. J Neurol 262:1493-503.

Ernster L, Schatz G (1981) Mitochondria: a historical review. J Cell Biol 91:227s-55s.

Estabrook RW (1967) Mitochondrial respiratory control and the polarographic measurement of ADP:O ratios. Methods Enzymol 10:41-7.

Faber C, Zhu ZJ, Castellino S, Wagner DS, Brown RH, Peterson RA, Gates L, Barton J, Bickett M, Hagerty L, Kimbrough C, Sola M, Bailey D, Jordan H, Elangbam CS (2014) Cardiolipin profiles as a potential biomarker of mitochondrial health in diet-induced obese mice subjected to exercise, diet-restriction and ephedrine treatment. J Appl Toxicol 34:1122-9.

Fell D (1997) Understanding the control of metabolism. Portland Press.

Forstner H, Gnaiger E (1983) Calculation of equilibrium oxygen concentration. In: Polarographic Oxygen Sensors. Aquatic and Physiological Applications. Gnaiger E, Forstner H (eds), Springer, Berlin, Heidelberg, New York:321-33.

Garlid KD, Beavis AD, Ratkje SK (1989) On the nature of ion leaks in energy-transducing membranes. Biochim Biophys Acta 976:109-20.

Garlid KD, Semrad C, Zinchenko V. Does redox slip contribute significantly to mitochondrial respiration? In: Schuster S, Rigoulet M, Ouhabi R, Mazat J-P, eds (1993) Modern trends in biothermokinetics. Plenum Press, New York, London:287-93.

Gerö D, Szabo C (2016) Glucocorticoids suppress mitochondrial oxidant production via upregulation of uncoupling protein 2 in hyperglycemic endothelial cells. PLoS One 11:e0154813.

Gnaiger E. Efficiency and power strategies under hypoxia. Is low efficiency at high glycolytic ATP production a paradox? In: Surviving Hypoxia: Mechanisms of Control and Adaptation. Hochachka PW, Lutz PL, Sick T, Rosenthal M, Van den Thillart G, eds (1993a) CRC Press, Boca Raton, Ann Arbor, London, Tokyo:77-109.

Gnaiger E (1993b) Nonequilibrium thermodynamics of energy transformations. Pure Appl Chem 65:1983-2002.

Gnaiger E (2001) Bioenergetics at low oxygen: dependence of respiration and phosphorylation on oxygen and adenosine diphosphate supply. Respir Physiol 128:277-97.

Gnaiger E (2009) Capacity of oxidative phosphorylation in human skeletal muscle. New perspectives of mitochondrial physiology. Int J Biochem Cell Biol 41:1837-45.

Gnaiger E (2014) Mitochondrial pathways and respiratory control. An introduction to OXPHOS analysis. 4th ed. Mitochondr Physiol Network 19.12. Oroboros MiPNet Publications, Innsbruck:80 pp.

1694   Gnaiger E, Méndez G, Hand SC (2000) High phosphorylation efficiency and depression of uncoupled respiration
1695   in mitochondria under hypoxia. Proc Natl Acad Sci USA 97:11080-5.
1696   Greggio C, Jha P, Kulkarni SS, Lagarrigue S, Broskey NT, Boutant M, Wang X, Conde Alonso S, Ofori E,
1697   Auwerx J, Cantó C, Amati F (2017) Enhanced respiratory chain supercomplex formation in response to
1698   exercise in human skeletal muscle. Cell Metab 25:301-11.
1699   Hinkle PC (2005) P/O ratios of mitochondrial oxidative phosphorylation. Biochim Biophys Acta 1706:1-11.
1700   Hofstadter DR (1979) Gödel, Escher, Bach: An eternal golden braid. A metaphorical fugue on minds and
1701   machines in the spirit of Lewis Carroll. Harvester Press:499 pp.
1702   Illaste A, Laasmaa M, Peterson P, Vendelin M (2012) Analysis of molecular movement reveals latticelike
1703   obstructions to diffusion in heart muscle cells. Biophys J 102:739-48.
1704   Jasienski M, Bazzaz FA (1999) The fallacy of ratios and the testability of models in biology. Oikos 84:321-26.
1705   Jepihhina N, Beraud N, Sepp M, Birkedal R, Vendelin M (2011) Permeabilized rat cardiomyocyte response
1706   demonstrates intracellular origin of diffusion obstacles. Biophys J 101:2112-21.
1707   Klepinin A, Ounpuu L, Guzun R, Chekulayev V, Timohhina N, Tepp K, Shevchuk I, Schlattner U, Kaambre T
1708   (2016) Simple oxygraphic analysis for the presence of adenylate kinase 1 and 2 in normal and tumor cells. J
1709   Bioenerg Biomembr 48:531-48.
1710   Klingenberg M (2017) UCP1 - A sophisticated energy valve. Biochimie 134:19-27.
1711   Koit A, Shevchuk I, Ounpuu L, Klepinin A, Chekulayev V, Timohhina N, Tepp K, Puurand M,Truu L, Heck K,
1712   Valvere V, Guzun R, Kaambre T (2017) Mitochondrial respiration in human colorectal and breast cancer
1713   clinical material is regulated differently. Oxid Med Cell Longev 1372640.
1714   Komlódi T, Tretter L (2017) Methylene blue stimulates substrate-level phosphorylation catalysed by succinyl-
1715   CoA ligase in the citric acid cycle. Neuropharmacology 123:287-98.
1716   Lane N (2005) Power, sex, suicide: mitochondria and the meaning of life. Oxford University Press:354 pp.
1717   Larsen S, Nielsen J, Neigaard Nielsen C, Nielsen LB, Wibrand F, Stride N, Schroder HD, Boushel RC, Helge
1718   JW, Dela F, Hey-Mogensen M (2012) Biomarkers of mitochondrial content in skeletal muscle of healthy
1719   young human subjects. J Physiol 590:3349-60.
1720   Lee C, Zeng J, Drew BG, Sallam T, Martin-Montalvo A, Wan J, Kim SJ, Mehta H, Hevener AL, de Cabo R,
1721   Cohen P (2015) The mitochondrial-derived peptide MOTS-c promotes metabolic homeostasis and reduces
1722   obesity and insulin resistance. Cell Metab 21:443-54.
1723   Lee SR, Kim HK, Song IS, Youm J, Dizon LA, Jeong SH, Ko TH, Heo HJ, Ko KS, Rhee BD, Kim N, Han J
1724   (2013) Glucocorticoids and their receptors: insights into specific roles in mitochondria. Prog Biophys Mol
1725   Biol 112:44-54.
1726   Leek BT, Mudaliar SR, Henry R, Mathieu-Costello O, Richardson RS (2001) Effect of acute exercise on citrate
1727   synthase activity in untrained and trained human skeletal muscle. Am J Physiol Regul Integr Comp Physiol
1728   280:R441-7.
1729   Lemieux H, Blier PU, Gnaiger E (2017) Remodeling pathway control of mitochondrial respiratory capacity by
1730   temperature in mouse heart: electron flow through the Q-junction in permeabilized fibers. Sci Rep 7:2840.
1731   Lenaz G, Tioli G, Falasca AI, Genova ML (2017) Respiratory supercomplexes in mitochondria. In: Mechanisms
1732   of primary energy trasduction in biology. M Wikstrom (ed) Royal Society of Chemistry Publishing, London,
1733   UK:296-337.
1734   Liu S, Roellig DM, Guo Y, Li N, Frace MA, Tang K, Zhang L, Feng Y, Xiao L (2016) Evolution of mitosome
1735   metabolism and invasion-related proteins in *Cryptosporidium*. BMC Genomics 17:1006.
1736   Margulis L (1970) Origin of eukaryotic cells. New Haven: Yale University Press.
1737   Meinild Lundby AK, Jacobs RA, Gehrig S, de Leur J, Hauser M, Bonne TC, Flück D, Dandanell S, Kirk N,
1738   Kaech A, Ziegler U, Larsen S, Lundby C (2018) Exercise training increases skeletal muscle mitochondrial
1739   volume density by enlargement of existing mitochondria and not de novo biogenesis. Acta Physiol 222,
1740   e12905.
1741   Menshikova EV, Ritov VB, Fairfull L, Ferrell RE, Kelley DE, Goodpaster BH (2006) Effects of exercise on
1742   mitochondrial content and function in aging human skeletal muscle. J Gerontol A Biol Sci Med Sci 61:534-
1743   40.
1744   Menshikova EV, Ritov VB, Ferrell RE, Azuma K, Goodpaster BH, Kelley DE (2007) Characteristics of skeletal
1745   muscle mitochondrial biogenesis induced by moderate-intensity exercise and weight loss in obesity. J Appl
1746   Physiol (1985) 103:21-7.
1747   Menshikova EV, Ritov VB, Toledo FG, Ferrell RE, Goodpaster BH, Kelley DE (2005) Effects of weight loss
1748   and physical activity on skeletal muscle mitochondrial function in obesity. Am J Physiol Endocrinol Metab
1749   288:E818-25.
1750   Miller GA (1991) The science of words. Scientific American Library New York:276 pp.
1751   Mitchell P (1961) Coupling of phosphorylation to electron and hydrogen transfer by a chemi-osmotic type of
1752   mechanism. Nature 191:144-8.
1753   Mitchell P (2011) Chemiosmotic coupling in oxidative and photosynthetic phosphorylation. Biochim Biophys
1754   Acta Bioenergetics 1807:1507-38.

Mogensen M, Sahlin K, Fernström M, Glintborg D, Vind BF, Beck-Nielsen H, Højlund K (2007) Mitochondrial respiration is decreased in skeletal muscle of patients with type 2 diabetes. Diabetes 56:1592-9.

Mohr PJ, Phillips WD (2015) Dimensionless units in the SI. Metrologia 52:40-7.

Moreno M, Giacco A, Di Munno C, Goglia F (2017) Direct and rapid effects of 3,5-diiodo-L-thyronine (T2). Mol Cell Endocrinol 7207:30092-8.

Morrow RM, Picard M, Derbeneva O, Leipzig J, McManus MJ, Gouspillou G, Barbat-Artigas S, Dos Santos C, Hepple RT, Murdock DG, Wallace DC (2017) Mitochondrial energy deficiency leads to hyperproliferation of skeletal muscle mitochondria and enhanced insulin sensitivity. Proc Natl Acad Sci U S A 114:2705-10.

Murley A, Nunnari J (2016) The emerging network of mitochondria-organelle contacts. Mol Cell 61:648-53.

National Academies of Sciences, Engineering, and Medicine (2018) International coordination for science data infrastructure: Proceedings of a workshop—in brief. Washington, DC: The National Academies Press. doi: https://doi.org/10.17226/25015.

Palmfeldt J, Bross P (2017) Proteomics of human mitochondria. Mitochondrion 33:2-14.

Paradies G, Paradies V, De Benedictis V, Ruggiero FM, Petrosillo G (2014) Functional role of cardiolipin in mitochondrial bioenergetics. Biochim Biophys Acta 1837:408-17.

Pesta D, Gnaiger E (2012) High-Resolution Respirometry. OXPHOS protocols for human cells and permeabilized fibres from small biopsies of human muscle. Methods Mol Biol 810:25-58.

Pesta D, Hoppel F, Macek C, Messner H, Faulhaber M, Kobel C, Parson W, Burtscher M, Schocke M, Gnaiger E (2011) Similar qualitative and quantitative changes of mitochondrial respiration following strength and endurance training in normoxia and hypoxia in sedentary humans. Am J Physiol Regul Integr Comp Physiol 301:R1078–87.

Price TM, Dai Q (2015) The role of a mitochondrial progesterone receptor (PR-M) in progesterone action. Semin Reprod Med 33:185-94.

Puchowicz MA, Varnes ME, Cohen BH, Friedman NR, Kerr DS, Hoppel CL (2004) Oxidative phosphorylation analysis: assessing the integrated functional activity of human skeletal muscle mitochondria – case studies. Mitochondrion 4:377-85. Puntschart A, Claassen H, Jostarndt K, Hoppeler H, Billeter R (1995) mRNAs of enzymes involved in energy metabolism and mtDNA are increased in endurance-trained athletes. Am J Physiol 269:C619-25.

Quiros PM, Mottis A, Auwerx J (2016) Mitonuclear communication in homeostasis and stress. Nat Rev Mol Cell Biol 17:213-26.

Rackham O, Mercer TR, Filipovska A (2012) The human mitochondrial transcriptome and the RNA-binding proteins that regulate its expression. WIREs RNA 3:675–95.

Reichmann H, Hoppeler H, Mathieu-Costello O, von Bergen F, Pette D (1985) Biochemical and ultrastructural changes of skeletal muscle mitochondria after chronic electrical stimulation in rabbits. Pflugers Arch 404:1-9.

Renner K, Amberger A, Konwalinka G, Gnaiger E (2003) Changes of mitochondrial respiration, mitochondrial content and cell size after induction of apoptosis in leukemia cells. Biochim Biophys Acta 1642:115-23.

Rice DW, Alverson AJ, Richardson AO, Young GJ, Sanchez-Puerta MV, Munzinger J, Barry K, Boore JL, Zhang Y, dePamphilis CW, Knox EB, Palmer JD (2016) Horizontal transfer of entire genomes via mitochondrial fusion in the angiosperm *Amborella*. Science 342:1468-73.

Rich P (2003) Chemiosmotic coupling: The cost of living. Nature 421:583.

Rostovtseva TK, Sheldon KL, Hassanzadeh E, Monge C, Saks V, Bezrukov SM, Sackett DL (2008) Tubulin binding blocks mitochondrial voltage-dependent anion channel and regulates respiration. Proc Natl Acad Sci USA 105:18746-51.

Rustin P, Parfait B, Chretien D, Bourgeron T, Djouadi F, Bastin J, Rötig A, Munnich A (1996) Fluxes of nicotinamide adenine dinucleotides through mitochondrial membranes in human cultured cells. J Biol Chem 271:14785-90.

Saks VA, Veksler VI, Kuznetsov AV, Kay L, Sikk P, Tiivel T, Tranqui L, Olivares J, Winkler K, Wiedemann F, Kunz WS (1998) Permeabilised cell and skinned fiber techniques in studies of mitochondrial function in vivo. Mol Cell Biochem 184:81-100.

Salabei JK, Gibb AA, Hill BG (2014) Comprehensive measurement of respiratory activity in permeabilized cells using extracellular flux analysis. Nat Protoc 9:421-38.

Sazanov LA (2015) A giant molecular proton pump: structure and mechanism of respiratory complex I. Nat Rev Mol Cell Biol 16:375-88.

Schneider TD (2006) Claude Shannon: biologist. The founder of information theory used biology to formulate the channel capacity. IEEE Eng Med Biol Mag 25:30-3.

Schönfeld P, Dymkowska D, Wojtczak L (2009) Acyl-CoA-induced generation of reactive oxygen species in mitochondrial preparations is due to the presence of peroxisomes. Free Radic Biol Med 47:503-9.

Schultz J, Wiesner RJ (2000) Proliferation of mitochondria in chronically stimulated rabbit skeletal muscle--transcription of mitochondrial genes and copy number of mitochondrial DNA. J Bioenerg Biomembr 32:627-34.

Speijer D (2016) Being right on Q: shaping eukaryotic evolution. Biochem J 473:4103-27.

Sugiura A, Mattie S, Prudent J, McBride HM (2017) Newly born peroxisomes are a hybrid of mitochondrial and ER-derived pre-peroxisomes. Nature 542:251-4.

Simson P, Jepihhina N, Laasmaa M, Peterson P, Birkedal R, Vendelin M (2016) Restricted ADP movement in cardiomyocytes: Cytosolic diffusion obstacles are complemented with a small number of open mitochondrial voltage-dependent anion channels. J Mol Cell Cardiol 97:197-203.

Stucki JW, Ineichen EA (1974) Energy dissipation by calcium recycling and the efficiency of calcium transport in rat-liver mitochondria. Eur J Biochem 48:365-75.

Tonkonogi M, Harris B, Sahlin K (1997) Increased activity of citrate synthase in human skeletal muscle after a single bout of prolonged exercise. Acta Physiol Scand 161:435-6.

Torralba D, Baixauli F, Sánchez-Madrid F (2016) Mitochondria know no boundaries: mechanisms and functions of intercellular mitochondrial transfer. Front Cell Dev Biol 4:107. eCollection 2016.

Vamecq J, Schepers L, Parmentier G, Mannaerts GP (1987) Inhibition of peroxisomal fatty acyl-CoA oxidase by antimycin A. Biochem J 248:603-7.

Waczulikova I, Habodaszova D, Cagalinec M, Ferko M, Ulicna O, Mateasik A, Sikurova L, Ziegelhöffer A (2007) Mitochondrial membrane fluidity, potential, and calcium transients in the myocardium from acute diabetic rats. Can J Physiol Pharmacol 85:372-81.

Wagner BA, Venkataraman S, Buettner GR (2011) The rate of oxygen utilization by cells. Free Radic Biol Med 51:700-712.

Wang H, Hiatt WR, Barstow TJ, Brass EP (1999) Relationships between muscle mitochondrial DNA content, mitochondrial enzyme activity and oxidative capacity in man: alterations with disease. Eur J Appl Physiol Occup Physiol 80:22-7.

Watt IN, Montgomery MG, Runswick MJ, Leslie AG, Walker JE (2010) Bioenergetic cost of making an adenosine triphosphate molecule in animal mitochondria. Proc Natl Acad Sci U S A 107:16823-7.

Weibel ER, Hoppeler H (2005) Exercise-induced maximal metabolic rate scales with muscle aerobic capacity. J Exp Biol 208:1635–44.

White DJ, Wolff JN, Pierson M, Gemmell NJ (2008) Revealing the hidden complexities of mtDNA inheritance. Mol Ecol 17:4925–42.

Wikström M, Hummer G (2012) Stoichiometry of proton translocation by respiratory complex I and its mechanistic implications. Proc Natl Acad Sci U S A 109:4431-6.

Williams EG, Wu Y, Jha P, Dubuis S, Blattmann P, Argmann CA, Houten SM, Amariuta T, Wolski W, Zamboni N, Aebersold R, Auwerx J (2016) Systems proteomics of liver mitochondria function. Science 352 (6291):aad0189

Willis WT, Jackman MR, Messer JI, Kuzmiak-Glancy S, Glancy B (2016) A simple hydraulic analog model of oxidative phosphorylation. Med Sci Sports Exerc 48:990-1000.